pubs.acs.org/acschemicalbiology

Perspective

Maximizing the Accuracy of Equilibrium Dissociation Constants for Affinity Complexes: From Theory to Practical Recommendations

Tong Ye Wang, Jean-Luc Rukundo, Zhiyuan Mao, and Sergey N. Krylov*

Cite This: *ACS Chem. Biol.* 2024, 19, 1852−1867

Read Online

ACCESS | Metrics & More | Article Recommendations | Supporting Information

ABSTRACT: The equilibrium dissociation constant (K_d) is a major characteristic of affinity complexes and one of the most frequently determined physicochemical parameters. Despite its significance, the values of K_d obtained for the same complex under similar conditions often exhibit considerable discrepancies and sometimes vary by orders of magnitude. These inconsistencies highlight the susceptibility of K_d determination to large systematic errors, even when random errors are small. It is imperative to both minimize and quantitatively assess the systematic errors inherent in K_d determination. Traditionally, K_d values are determined through nonlinear regression of binding isotherms. This analysis utilizes three variables: concentrations of two reactants and a fraction R of unbound limiting reactant. The systematic errors in K_d arise directly from systematic errors in these variables. Therefore, to maximize the accuracy of K_d, this study thoroughly analyzes the sources of systematic errors within the three variables, including (*i*) non-additive signals to calculate R, (*ii*) mis-calibrated experimental instruments, (*iii*) inaccurate calibration parameters, (*iv*) insufficient incubation time, (*v*) unsaturated binding isotherm, (*vi*) impurities in the reactants, and (*vii*) solute adsorption onto surfaces. Through this analysis, we illustrate how each source contributes to inaccuracies in the determination of K_d and propose strategies to minimize these contributions. Additionally, we introduce a method for quantitatively assessing the confidence intervals of systematic errors in concentrations, a crucial step toward quantitatively evaluating the accuracy of K_d. While presenting original findings, this paper also reiterates the fundamentals of K_d determination, hence guiding researchers across all proficiency levels. By shedding light on the sources of systematic errors and offering strategies for their mitigation, our work will help researchers enhance the accuracy of K_d determination, thereby making binding studies more reliable and the conclusions drawn from such studies more robust.

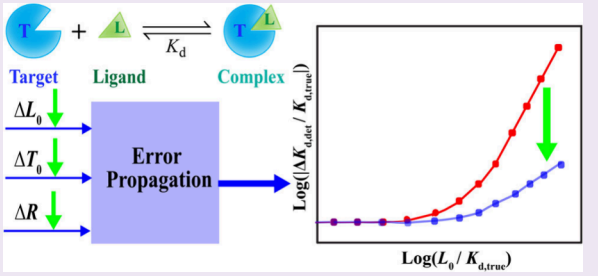

Downloaded via Sergey Krylov on September 4, 2025 at 21:49:34 (UTC).
See https://pubs.acs.org/sharingguidelines for options on how to legitimately share published articles.

1. INTRODUCTION

The equilibrium dissociation constants (K_d) of affinity complexes drive important decisions, such as ranking drug leads and choosing prevailing mechanisms in cellular regulation.[1−5] Correct decisions require accurate K_d values, but K_d values determined for the same complex under similar conditions often differ from each other by folds or even orders of magnitude while having small relative standard deviations (i.e., random errors).[6,7] Such substantial differences suggest that K_d determination is subject to large systematic errors, or in other words, is inherently inaccurate.

A determined K_d value ($K_{d,det}$) always differs from the true value of K_d ($K_{d,true}$), and systematic error in $K_{d,det}$ (ΔK_d) is defined as

$$\Delta K_{d,det} = K_{d,det} - K_{d,true} \quad (1)$$

Since the true value of K_d is fundamentally unknown, the systematic error of $K_{d,det}$ cannot be found using this definition. Therefore, the question of "how accurate is the determined value of K_d?" lacks a definite quantitative answer. Our inability to quantitatively characterize the accuracy of $K_{d,det}$ underscores the imperative to implement all available measures aimed at improving this accuracy, or in the other words, minimizing the systematic error in $K_{d,det}$.

The ramifications of inaccuracies in K_d determination are profound. Inaccurate K_d values can distort the ranking of drug leads, potentially prioritizing low-potency compounds over high-potency ones, thereby compromising the efficacy of R&D efforts in drug discovery.[7−11] Moreover, inaccurate K_d values can lead to misinterpretation of biological data and perpetuate fundamental misconceptions in biological research for extended periods.[7,12,13] It is crucial to emphasize the necessity of accurate K_d determination, which unfortunately remains a challenge.

Over the past decade, notable works and practical guidelines have been developed to help researchers improve the accuracy of experimentally determined K_d values.[14−16] Despite this, only

Received: April 15, 2024
Revised: July 31, 2024
Accepted: August 5, 2024
Published: August 9, 2024

ACS Publications

© 2024 American Chemical Society

https://doi.org/10.1021/acschembio.4c00259
ACS Chem. Biol. 2024, 19, 1852−1867

a small portion of studies adhere to these established guidelines,[14] primarily due to two reasons. First, many experimentalists are unaware of how significantly systematic errors in variables (e.g., concentrations) can affect the accuracy of K_d determination. Second, implementing the recommended measures, such as constructing multiple binding isotherms with varying incubation times and concentrations of the limiting component, is both time-consuming and resource-intensive. The lack of adherence to established guidelines has motivated us to conduct a systematic theoretical study aimed at (*i*) identifying fundamental determinants of K_d accuracy,[17] (*ii*) quantitatively demonstrating the importance of eliminating common sources of systematic errors and providing guidance for doing so, (*iii*) developing a practical approach for assessing the accuracy of experimentally determined K_d from a single binding isotherm,[18] and, ultimately, and (*iv*) establishing consensus standard requirements for binding experiments by the broader research community.[19] Here we focus on the second aspect.

A classic way to determine K_d includes two major steps (Figure 1A).[20−23] Step 1 is experimentally building a binding

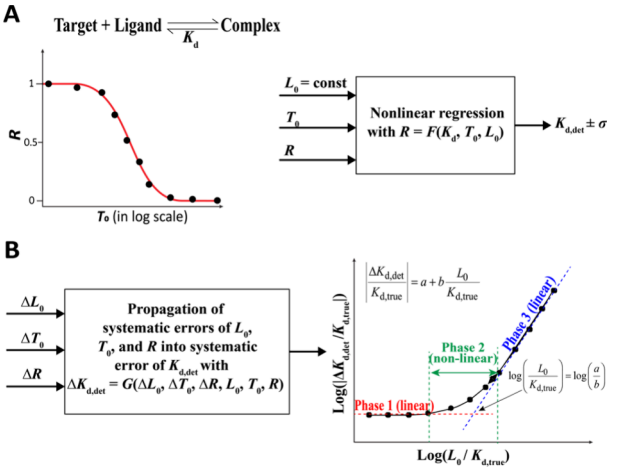

Figure 1. Schematic representations of A) determination of K_d and its standard deviation (σ) by nonlinear regression with three variables from the binding isotherm (L_0, T_0, and R) and B) propagation of systematic errors in these variables leading to a triphasic dependence of the relative systematic error in $K_{d,det}$ on the ratio $L_0/K_{d,true}$. (The right subpanel of panel B is modified with permission from ref 17. Copyright 2023 American Chemical Society.)

isotherm using a set of equilibrium mixtures containing two components: a limiting component, which we term ligand (L), and an excess component, which we term target (T). The ligand is kept at a constant total concentration L_0 across all equilibrium mixtures while the total concentration of the target T_0 is varied from mixture to mixture in a wide range. A binding isotherm is the dependence of a fraction R of unbound (or bound) ligand on T_0 at a constant L_0.

Step 2 in K_d determination is nonlinear regression of the binding isotherm with a known regression model, $R = F(L_0, T_0, K_d)$, derived from the definitions of R and K_d as well as mass balance for ligand, target, and complex. In this regression procedure, K_d is an unknown sought parameter, L_0 and T_0 are known independent variables, and R is a known dependent variable. The result of nonlinear regression is a determined K_d value and its standard deviation (random error) σ obtained under the assumption that all three variables (L_0, T_0, and R) are subject to random errors only. The value of σ describes the precision of $K_{d,det}$ but suggests nothing about the accuracy of $K_{d,det}$.[24,25] In other words, the probability of the $K_{d,true}$ to be found inside of the $K_{d,det} \pm \sigma$ range is unknown and can be very low.

As K_d is not measured directly but determined using nonlinear regression with a known regression model, the accuracy of $K_{d,det}$ is defined by the accuracy of the three variables (L_0, T_0, and R) (Figure 1B).[17] Note, the use of an incorrect regression model will lead to inaccurate $K_{d,det}$ even if L_0, T_0, and R are free of systematic errors. Using error propagation rules, we can link the systematic error in $K_{d,det}$ to systematic errors in L_0, T_0, and R: $\Delta K_{d,det} = G(\Delta L_0, \Delta T_0, \Delta R, L_0, T_0, R)$. The dependence of $\Delta K_{d,det}$ on L_0 is such that when L_0 is much greater than the unknown $K_{d,true}$ value, then the relative systematic error in $K_{d,det}$ is equal to a combination of relative systematic errors in the variable multiplied by $L_0/K_{d,true}$.[17] Decreasing systematic errors in $K_{d,det}$ thus requires decreasing both L_0 and systematic errors in the variables. As decreasing L_0 is restricted by limits of quantitation (LOQ) of instruments,[17] decreasing systematic errors in variables is viewed as an effective way of improving the accuracy of K_d determination.

Minimizing the systematic error in $K_{d,det}$ is an important task which can be translated into minimizing systematic errors in the variables. The drawback of such minimization is that it is blind; we minimize the error without knowing its value. The limitation of blind minimization is that even if all known precautions are taken to minimize systematic errors in variables (and, thus, in $K_{d,det}$), the resulting $K_{d,det}$ may still be insufficiently accurate for an intended application, but we will not know that. The major problem, which is not directly addressed in this work, is the lack of a practical approach for researchers who routinely determine K_d values to quantitatively assess the accuracy of $K_{d,det}$. Some numerical statistical methods, such as bootstrapping and Bayesian analysis, exist for assessing confidence intervals of parameters determined through nonlinear regression.[26−28] However, these methods are very rarely utilized by molecular scientists particularly due to the ambiguity associated with the inputs, which are confidence intervals of variables. Thus, we started the presented work with two goals in mind: (*i*) minimization of systematic errors in variables and (*ii*) quantitative assessment of the confidence intervals of the variables. Accordingly, after providing the required theoretical background on K_d determination and error propagation, we analyze major sources of systematic errors in variables R, L_0, and T_0, and we also identify means of minimizing these errors and study how their confidence intervals can be quantitatively assessed.

This work represents a rigorous examination of the universal sources of systematic errors in K_d determination using equilibrium methods. As such, it serves as an indispensable resource for researchers conducting binding studies by offering detailed insights and practical methodologies to significantly enhance the accuracy of K_d determinations. Furthermore, we anticipate that this work will lay the groundwork for incorporating K_d accuracy considerations into undergraduate and graduate curricula focused on binding methods. Additionally, it will support reviewers and editors in assessing the rigor and adequacy of experiments reported in scientific publications that present K_d values. By providing a comprehensive analysis and practical guidelines, this study aims to elevate research

https://doi.org/10.1021/acschembio.4c00259
ACS Chem. Biol. 2024, 19, 1852−1867

standards in this field, ensuring more reliable and reproducible results, ultimately benefiting the broader scientific community.

2. THEORETICAL BACKGROUND

2.1. Binding Process. Since the considerations of stoichiometry and cooperativity of binding would greatly complicate this study, here we only consider a simple 1:1 binding process between a target and a ligand, which is the most abundant type of interactions in biological and technological contexts:[15,29,30]

$$\text{Target} + \text{Ligand} \underset{k_{off}}{\overset{k_{on}}{\rightleftarrows}} \text{Complex} \tag{2}$$

Here k_{on} and k_{off} are rate constants of complex formation and dissociation, respectively. K_d can be defined through either these rate constants or equilibrium concentrations of the target (T), ligand (L), and complex (C), as follows:

$$K_d = \frac{k_{off}}{k_{on}} = \frac{TL}{C} \tag{3}$$

Lower K_d values correspond to higher thermodynamic stability of the complex. The equilibrium concentrations are linked to each other through the formal total concentrations of the target (T_0) and ligand (L_0) according to the rules of mass balance:

$$T_0 = T + C, \quad L_0 = L + C \tag{4}$$

T_0 and L_0 are concentrations of target and ligand, respectively, after mixing solutions of these two reactants but before any complex is formed. Experimentally, T, L, and C cannot be directly measured to determine the K_d. However, K_d can be calculated with known T_0, L_0, and fraction of unbound ligand R; the latter links K_d to T_0 and L_0.

2.2. Fraction *R* of Unbound Ligand. The determination of K_d requires experimentally finding a fraction R of target-unbound ligand (or a fraction of target-bound ligand, $1 - R$), in the equilibrium mixture of the target and ligand:

$$R = \frac{L}{L_0} \tag{5}$$

The general procedure for finding R starts with preparing the equilibrium mixture of the ligand and target. The procedure is facilitated by the physical or spectral separation of the unbound ligands from the complex. The separation is complete if the peaks or spectra of the unbound ligand and the complex do not overlap; otherwise, it is incomplete. The choice of a signal-processing approach depends on whether or not the separation is complete.

Complete separation of the unbound ligand from the target−ligand complex allows one to measure two signals from the equilibrium mixture — one is a signal from the unbound ligand (S_L) and the other is a signal from the target−ligand complex (S_C) — and express R using the two signals:[22,31,32]

$$R = \frac{L}{L_0} = \frac{S_L}{S_L + S_C/\varphi} \tag{6}$$

where φ is a factor by which the signal of ligand changes when it binds the target, e.g., in the case of fluorescence detection, φ is the quantum yield of the target-bound ligand relative to that of the unbound ligand.

Only a cumulative signal S from the unbound ligand and the target-bound ligand in the equilibrium mixture can be measured when their separation is incomplete. Typically, R is determined using additive signals (signal additivity is explained in detail in Note S1), which satisfy the principle of superposition:[21,23,33,34]

$$S = S_L^* \frac{L}{L_0} + S_C^* \frac{C}{L_0} \tag{7}$$

where S_L* and S_C* are signals from equimolar concentrations of pure ligand and pure complex and S is a signal from a mixture containing both unbound ligand and complex of a total concentration equal to that used to measure S_L* and S_C*. Note that, signal being linearly dependent on concentration is a sufficient condition for the establishment of eq 7 (Note S2). In the case of incomplete separation of signals from the unbound and target-bound signals, the value of R can still be determined, but three signals, S, S_C*, and S_L*, are required instead of two signals in eq 6:[21,23,33,35]

$$R = \frac{S - S_C^*}{S_L^* - S_C^*} \tag{8}$$

Measuring signal S for the mixture is trivial. Measuring signal S_L* for pure ligand is also trivial as S_L* is the signal from the ligand in the absence of target. Measuring signal S_C* from the pure complex in the case of incomplete separation requires that $C \gg L$, which is achieved via using a saturating total concentration of the target in the equilibrium mixture:

$$T_0 > L_0, \quad T_0 \gg K_{d,true} \tag{9}$$

It is hard to ensure the second inequality is satisfied as $K_{d,true}$ in fundamentally unknown. Moreover, target solubility and a significant increase in viscosity of the sample due to excessively high T_0 may limit the ability to find S_C*. Accordingly, complete separation of the free and target-bound ligands is preferable to incomplete separation.

2.3. General Approach to K_d Determination. There are two major ways to find K_d when R has been determined. In the first way, a formula that explicitly relates K_d to R is used:[36]

$$K_d = \frac{T_0 - L_0(1 - R)}{(1/R - 1)} \tag{10}$$

This formula is obtained by solving eq 3 using mass balance equations for both ligand and target (eq 4), and the definition of R (eq 5). This approach requires a single value of R. Calculation of K_d with this formula is most accurate for R approximately equal to 1/2.[22] However, K_d values determined this way are very sensitive to random errors of R, T_0, and L_0, especially when R is closer to zero or unity than to 1/2 (Note S3). Therefore, an alternative approach, which relies on nonlinear regression is typically used.

In the nonlinear-regression approach, K_d is determined by using multiple values of R found for a constant value of L_0 but different values of T_0. The dependence of R on T_0 is called a binding isotherm, which exhibits a characteristic sigmoidal shape in a semilogarithmic presentation of the isotherm (dots in Figure 1). K_d is then computed by fitting the binding isotherm with a theoretical dependence of R on T_0 (aka, nonlinear regression model) while using K_d as a fitting parameter. A correct model can be obtained by solving eq 10 for R without any simplifying assumption:[19,20,32]

https://doi.org/10.1021/acschembio.4c00259
ACS Chem. Biol. 2024, 19, 1852−1867

$$R = -\frac{K_d + T_0 - L_0}{2L_0} + \sqrt{\left(\frac{K_d + T_0 - L_0}{2L_0}\right)^2 + \frac{K_d}{L_0}} \quad (11)$$

An example of the best fit of a binding isotherm obtained with eq 11 is shown as a red line in Figure 1. In the nonlinear-regression procedure, K_d is a determined parameter, L_0 and T_0 are independent variables, and R is a dependent variable.

The regression model presented by eq 11 (as well as other regression models) assumes that only random errors are present in the variables, i.e., R, T_0, and L_0. Those errors result in a random error of $K_{d,det}$ which is reported at the output of nonlinear regression as a standard deviation σ. The standard deviation (σ) of $K_{d,det}$ along with the mean value of $K_{d,det}$ indicates the precision of $K_{d,det}$. Importantly, it is not necessary to repeat the determination of R for the same value of T_0 to assess the random error of $K_{d,det}$.

If any of R, T_0, or L_0 has a systematic error, then K_d cannot be determined accurately with a model presented by eq 11. Furthermore, if systematic errors exist in R, T_0, or L_0 and their magnitudes are unknown, then not only is $K_{d,det}$ inaccurate, but also the systematic error in $K_{d,det}$ remains unknown. On the other hand, if some information about the accuracy of R, T_0, or L_0 is known then the correct regression model presented by eq 11 can, in principle, help assess the accuracy of $K_{d,det}$.[18,26−28]

2.4. Propagation of Systematic Errors. The accuracy of $K_{d,det}$ depends on the accuracies of L_0, T_0, and R. If the values of L_0, T_0, and R were known accurately (i.e., had no systematic errors), then K_d determination would be accurate (e.g., subject to random errors only). However, this is not the case, and systematic errors in L_0, T_0, and R (designated as ΔL_0, ΔT_0, and ΔR) always exist and translate to the systematic error in $K_{d,det}$ (designated as $\Delta K_{d,det}$) as explained below assuming (for now) that ΔL_0, ΔT_0, and ΔR are known.

The manner in which ΔL_0, ΔT_0, and ΔR are translated into $\Delta K_{d,det}$ is governed by the error-propagation rules. Such rules, in turn, depend (though not critically) on whether ΔL_0, ΔT_0, and ΔR are strongly or weakly correlated. If they are strongly correlated (which will be the case if similar procedures are used for the preparation of solutions of ligand and target, and ΔR is solely the consequence of ΔL_0 and ΔT_0), then we can approximate the absolute value of $\Delta K_{d,det}$ by the following expression based on the using of error-propagation rule for fully correlated errors:

$$|\Delta K_{d,det}| = \left|\left(\frac{\partial K_d}{\partial T_0}\right)\Delta T_0\right| + \left|\left(\frac{\partial K_d}{\partial L_0}\right)\Delta L_0\right| + \left|\left(\frac{\partial K_d}{\partial R}\right)\Delta R\right| \quad (12)$$

We can apply eq 12 to the dependence of K_d on L_0, T_0, and R (eq 10) and obtain[17]

$$\left|\frac{\Delta K_{d,det}}{K_{d,true}}\right| = a + b\frac{L_0}{K_{d,true}} \quad (13)$$

where a is a constant depending only on $|\Delta T_0/T_0|$ and $|\Delta R/R|$ while b is a constant depending on all three relative errors: $|\Delta T_0/T_0|$, $|\Delta L_0/L_0|$, and $|\Delta R/R|$.

If ΔL_0, ΔT_0, and ΔR are weakly correlated (which will be the case if different procedures are used for the preparation of solutions of ligand and target, and ΔR is independent of ΔL_0 and ΔT_0), then we can approximate the absolute value of $\Delta K_{d,det}$ by the following expression based on the use of the error-propagation rule for fully uncorrelated errors:

$$|\Delta K_{d,det}| = \sqrt{\left(\frac{\partial K_d}{\partial T_0}\right)^2 \Delta T_0{}^2 + \left(\frac{\partial K_d}{\partial L_0}\right)^2 \Delta L_0{}^2 + \left(\frac{\partial K_d}{\partial R}\right)^2 \Delta R^2} \quad (14)$$

We can apply eq 14 to the dependence of K_d on L_0, T_0, and R (eq 10) and obtain[17]

$$\left|\frac{\Delta K_{d,det}}{K_{d,true}}\right| = \sqrt{\alpha^2 + \lambda\frac{L_0}{K_d} + \beta^2\left(\frac{L_0}{K_{d,true}}\right)^2} \quad (15)$$

where α and λ are constants depending only on $|\Delta T_0/T_0|$ and $|\Delta R/R|$ while β is a constant depending on all three relative errors: $|\Delta T_0/T_0|$, $|\Delta L_0/L_0|$, and $|\Delta R/R|$. In propagating the errors to obtain eqs 13 and 15, a single simplifying assumption was made, that the determined (from measured signals) value of R is equal to 0.5, which leads to the least erroneous $K_{d,det}$.[17,22] Thus, we are considering the best-case scenario, and eqs 13 and 15 represent the lower limit for relative systematic errors in $K_{d,det}$. Exact dependencies of a and b as well as α, λ, and β on $|\Delta T_0/T_0|$, $|\Delta L_0/L_0|$, and $|\Delta R/R|$ are not important here but can be found elsewhere.[17]

Although eqs 13 and 15 appear different, they are similar in the triphasic shape of $|\Delta K_{d,det}/K_{d,true}|$ dependence on $L_0/K_{d,true}$ (Figure 1B). The first phase corresponds to low $L_0/K_{d,true}$ values and is linear with negligible dependence of $|\Delta K_{d,det}/K_{d,true}|$ on $L_0/K_{d,true}$. The reason for the first phase to be virtually parallel to the x-axis is that the first term prevails over the second in eq 13 and the first two terms prevail over the third term in eq 15 for low values of $L_0/K_{d,true}$. For phase 3, which corresponds to large $L_0/K_{d,true}$ values, eqs 13 and 15 approach another linear phase: $|\Delta K_{d,det}/K_{d,true}| = b(L_0/K_{d,true})$ and $|\Delta K_{d,det}/K_{d,true}| = \beta(L_0/K_{d,true})$, respectively; that phase shows a high sensitivity of $|\Delta K_{d,det}/K_{d,true}|$ to $L_0/K_{d,true}$. There is a nonlinear transition range (phase 2) between the two linear phases. Moreover, both eqs 13 and 15 suggest that the minimum $|\Delta K_{d,det}/K_{d,true}|$ value (in phase 1) depends on a single parameter (a in eq 13 or α in eq 15) that is defined only by $|\Delta T_0/T_0|$ and $|\Delta R/R|$, while the sensitivity of $|\Delta K_{d,det}/K_{d,true}|$ to $L_0/K_{d,true}$ in phase 3 mainly depends on a parameter (b in eq 13 or β in eq 15) that is defined by relative errors of all three variables: $|\Delta T_0/T_0|$, $|\Delta L_0/L_0|$, and $|\Delta R/R|$.

As suggested by eqs 13 and 15, to increase the accuracy of $K_{d,det}$ (i.e., to decrease $|\Delta K_{d,det}/K_{d,true}|$), one can decrease the ligand concentration L_0 (to reduce the $L_0/K_{d,true}$ ratio) and/or minimize the relative systematic errors in L_0, T_0, and R. Since L_0 cannot be lower than the LOQ of an instrument utilized for measuring signals (and, thus, finding the values of R),[17] it is not practical to decrease $L_0/K_{d,true}$ to a very low value in many cases, especially in the studies of very stable complexes (small values of $K_{d,true}$). Thus, understanding the sources of systematic errors in L_0, T_0, and R and how these errors influence the accuracy of $K_{d,det}$ is crucial for minimizing such systematic errors and further improving the accuracy of $K_{d,det}$.

3. RESULTS AND DISCUSSION

3.1. Effect of an Incorrect Regression Model on K_d Accuracy. Before considering sources of systematic errors in L_0, T_0, and R, we would like to demonstrate the importance of using a correct regression model (e.g., eq 11). It is common in

https://doi.org/10.1021/acschembio.4c00259
ACS Chem. Biol. 2024, 19, 1852−1867

the research community to fit binding isotherms with a simplified hyperbolic equation:[14−16]

$$R = \frac{K_d}{K_d + T_0} \tag{16}$$

This equation is derived from the definitions of K_d and R (eqs 3 and 5) and mass balance for ligand and target with assuming $T \approx T_0$.[14−16] Eq 16 is only applicable to K_d determination under the condition of $L_0 \ll K_{d,true}$;[14−16] however, since $K_{d,true}$ is fundamentally unknown and L_0 cannot be below the LOQ of the instrument, it is hard to ensure that the condition of $L_0 \ll K_{d,true}$ is achieved. In essence, despite the simplicity of eq 16, it is an incorrect (or inaccurate) regression model, and using it will necessarily result in systematic errors in $K_{d,det}$ even if L_0, T_0, and R are free of systematic errors. It is, therefore, instructive to demonstrate the extent of inaccuracy of $K_{d,det}$ caused by the use of eq 16 instead of eq 11 in nonlinear regression (Figure 2).

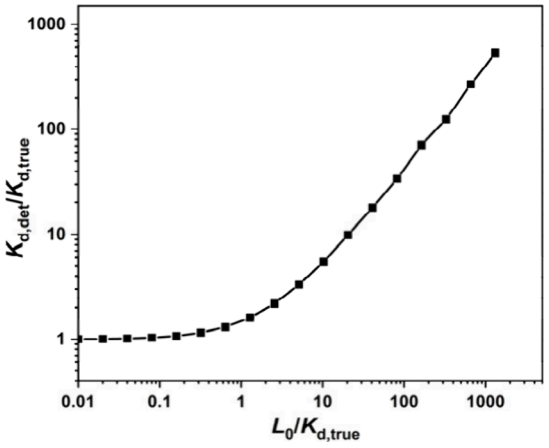

Figure 2. Dependence of $K_{d,det}/K_{d,true}$ on $L_0/K_{d,true}$ when using the simplified hyperbolic eq (eq 16) to fit the theoretical binding isotherms that were simulated with eq 11. There was no error added to L_0, T_0, and R.

Importantly, using eq 16 leads to an overestimation of $K_{d,det}$ and can result in $L_0 < K_{d,det}$ even when $L_0 > K_{d,true}$. This emphasizes the importance of not comparing L_0 to $K_{d,det}$, as it not only is incorrect but also can be misleading. Our results strongly suggest that the correct model (eq 11) should be used for nonlinear regression if both T_0 and L_0 are known. Exceptions include cases where determining what L_0 represents is challenging, making the use of eq 11 impossible.[14] Classic examples are methods with surface-immobilized ligand, such as BLI and SPR. Therefore, using the correct regression model is crucial for the accurate determination of K_d. Below, we will only use eq 11.

3.2. Sources of Systematic Errors in *R*. Systematic errors in $K_{d,det}$ can be attributed to systematic errors in R, which can originate from various sources. Here, we analyze four common sources of ΔR: (*i*) using non-additive signals to calculate R, (*ii*) using an uncalibrated signal-detection instrument or incorrectly determined calibration parameters in calculating R, (*iii*) using insufficient incubation time without allowing mixtures to reach equilibrium, and (*iv*) measuring S_C* (signal for pure complex) without satisfying saturation condition described in eq 9. Most of these error sources result from theoretical or experimental mistakes and should be addressed during the experimental design and preliminary experiments. Some other less common but well-studied error sources, such as disturbing equilibrium by (*i*) physical separation of the target−ligand complexes from the unreacted ligand and (*ii*) change of conditions (e.g., temperature) caused by detection, etc.,[15,37−41] are not presented and discussed in this work.

In this Perspective, we consider only the universal origins of inaccuracies in R. However, each method has its own specific sources of inaccuracies. While we do not delve into these method-specific sources, we strongly recommend that practitioners thoroughly study the limitations and potential inaccuracies associated with their chosen methods. Comprehensive analyses of these limitations and sources of inaccuracy are available in the literature for all widely used methods of K_d determination. Below, we provide references to some useful materials for several methods that we subjectively view as most widely used in the research community of Chemical Biologists: Enzyme-Linked Immuno-Sorbent Assays (ELISA),[42−44] Surface Plasmon Resonance (SPR),[45−47] Bio-Layer Interferometry (BLI),[48−50] Microscale Thermophoresis (MST),[51−53] Isothermal Titration Calorimetry (ITC),[54−56] and Nuclear Magnetic Resonance (NMR).[57−59]

3.2.1. Non-additive Signals. Systematic errors in R can arise from the use of a non-additive signal, which does not satisfy eq 7 and, accordingly, cannot be used in eq 8 (derived from eq 7) to calculate R. Examples of K_d-determination approaches using signals that have been proven to be additive/non-additive are shown in Table 1. Note that the additivity status of some signals listed in Table 1 is proven in this work, while we do not have such information for Back-Scattering Interferometry (BSI). Table 1 serves as a starting point for reviewing the additive characters of the signals used in various K_d-determination approaches. Researchers in the field of K_d determination are invited to comment on and/or correct this information on https://www.researchgate.net/post/Additivity_of_signals_used_in_Kd-determination_approaches, where we will upload the updated table regularly. Here, considering examples of non-additive signals within the context of specific K_d-determination approaches is instructive. Our results indicate that a signal should be proven to be additive before it can be used to calculate R. Otherwise, large systematic errors in $K_{d,det}$ might be caused by mistakenly using non-additive signals in R calculations.

3.2.1.1. Mobility-Based Methods. A method commonly used for K_d determination for relatively unstable complexes is based on mobilities of unbound ligand and target-bound ligand in capillary electrophoresis (CE).[60] In this method, a short plug of the ligand of concentration L_0 is injected into a capillary prefilled with the running buffer containing the target at a concentration of T_0. This plug of the ligand moves through the capillary by an electric field under the condition of pseudoequilibrium in binding process (eq 2) which is equivalent to a condition that the characteristic equilibration time (t_{eq}) is much smaller than the characteristic separation time (t_{sep}):

$$t_{eq} \ll t_{sep} \tag{17}$$

The characteristic equilibration time for a case of $T_0 \gg L_0$ can be approximated by[38]

$$t_{eq} \approx (k_{off} + k_{on}T_0)^{-1} \tag{18}$$

https://doi.org/10.1021/acschembio.4c00259
ACS Chem. Biol. 2024, 19, 1852−1867

Table 1. Examples of K_d-Determination Approaches with Information of Signals Used to Calculate R and Their Additivity

Approach	Signal	Additivity[a]	References with proof[b]	Supplementary references
Accurate Constant via Transient Incomplete Separation (ACTIS)	Fluorescence intensity	√	23	78, 79
	Ion-signal intensity	√		
Affinity Capillary Electrophoresis (ACE)	Electrophoretic mobility	√	63	60, 62
	Migration velocity (with constant mobility of electroosmotic flow)	√		
	Migration time	×	Section 3.2.1.1	N/A
Non-Equilibrium Capillary Electrophoresis of Equilibrium Mixtures (NECEEM)	Peak area	√	37	22, 90
Back-Scattering Interferometry (BSI)	Refractive index in solution	?	N/A	91, 92
Surface Plasmon Resonance (SPR)	Refractive index on surface	√	93	94−96
Bio-Layer Interferometry (BLI)	Wavelength shift	√	97	98, 99
Enzyme-Linked Immuno-Sorbent Assays (ELISA)	Absorbance	√	100	101, 102
Solid Phase Radio-Immuno-Assay (SPRIA)	Radioactivity	√	103	104, 105
Flow Induced Dispersion Analysis (FIDA)	Apparent diffusion coefficient	×	Section 3.2.1.3	72, 74
Taylor Dispersion Analysis (TDA)	Reciprocal of apparent diffusion coefficient	×	Section 3.2.1.3	106
Rotational Depolarization of Fluorescence	Anisotropy	√	67	64, 107
	Polarization	×	68, Note S4	108−110
Fluorescence Resonance Energy Transfer (FRET)	Fluorescence intensity	√	111	112
High-Performance Liquid Chromatography (HPLC)	Peak area	√	113	114
Isothermal Titration Calorimetry (ITC)	Binding enthalpy	√	115	116, 117
Microscale Thermophoresis (MST)	Fluorescence intensity	√	118	21
Native Mass Spectrometry (MS)	Ion signal intensity	√	119	120, 121
Nuclear Magnetic Resonance (NMR)	Chemical shift	√	122	7, 123, 124
	Longitudinal and transverse relaxation rates	×	125	126
Electrophoretic Mobility Shift Assay (EMSA)	Radioactivity or light/fluorescence intensity	√	127	128, 129
Gel Filtration	Absorbance	√	130	131

[a]Symbol "√" indicates that a proof of additivity exists, symbol "×" indicates that the proof of non-additivity exists, and symbol "?" indicates that the authors did not find a proof of additivity or non-additivity. [b]In some references, it is not directly shown that whether the measured signals satisfy eq 7 or not. In these cases, if the measured signal is proven to be proportional to the quantities (e.g., concentrations, layer thicknesses, etc.) of target-unbound and target-bound ligands, we consider that the additivity of the signal is proven (refer to discussion in Notes S1 and S2).

The characteristic separation time is

$$t_{sep} = \frac{l}{\min(|v_T - v_L|, |v_C - v_L|)} \quad (19)$$

where l is the length of the plug of ligand, and v_T, v_L, and v_C are velocities of the target, ligand, and complex, respectively. Usually, the complex moves with the velocity intermediate to those of the unbound ligand and target, that is $|v_C - v_L| < |v_T - v_L|$, and eq 19 can be written as

$$t_{sep} = \frac{l}{|v_C - v_L|} \quad (20)$$

The migration time of the peak of ligand to the detector t is a common measurable signal in capillary electrophoresis (CE),[61] but time is not additive, while if the mobility of electroosmotic flow is independent of T_0, the velocity and inverse migration time are both additive:[60,62,63]

$$v = v_L\frac{L}{L_0} + v_C\frac{C}{L_0}$$
$$\frac{1}{t} = \frac{1}{t_L}\frac{L}{L_0} + \frac{1}{t_C}\frac{C}{L_0} \quad (21)$$

Binding isotherms with both time and velocity as a signal have characteristic and undistinguishable sigmoidal shapes; however, they are shifted with respect to each other (Figure 3). If one wrongly uses time instead of inverse time to calculate R with eq 8, then the resulting $K_{d,det}$ will have significant systematic errors at both low and high $L_0/K_{d,true}$ values (Figure 3).

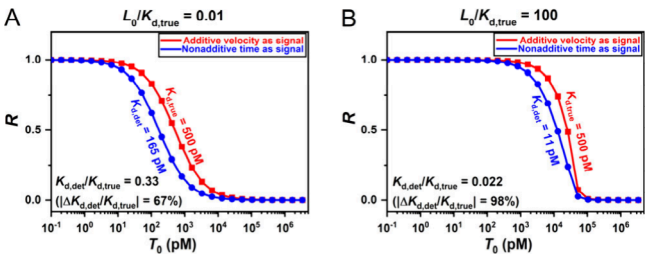

Figure 3. Comparison of the results produced by using the additive velocity (v) and non-additive time (t) as signals: binding isotherms and $K_{d,det}$ obtained with signals of velocity (red) and time (blue) for $L_0/K_{d,true}$ = 0.01 (A) and $L_0/K_{d,true}$ = 100 (B). In the simulation, the theoretical/input $K_{d,true}$ = 500 pM.

3.2.1.2. Methods Based on Fluorescence Anisotropy. Both fluorescence anisotropy (r) and polarization (P) are the parameters that quantitatively describe the degree of light polarization in different contexts.[64] Fluorescence anisotropy was introduced specifically to characterize light emitted by a fluorophore in three dimensions while polarization was introduced to characterize polarization of a beam of collimated light from a light source in a plane perpendicular to the beam. Thus, fluorescence anisotropy and beam-light polarization are applied to different dimensionalities which are reflected in formulas expressing r and P through the two component light intensities, factoring in the total light intensity.

https://doi.org/10.1021/acschembio.4c00259
ACS Chem. Biol. 2024, 19, 1852−1867

Fluorescence anisotropy is defined as follows:[64]

$$r = \frac{I_{\parallel} - I_{\perp}}{I_{\parallel} + 2I_{\perp}} \tag{22}$$

where $I_{\parallel}$ is the intensity of light emitted by a fluorophore with a polarization orientation parallel to that of the excitation light; $I_{\perp}$ is the intensity of emitted light with a polarization orientation perpendicular to that of the excitation light. The denominator of eq 22 contains a factor of 2 because there are two symmetrical dimensions perpendicular to the direction of excitation-light polarization, but only the intensity associated with one of them (i.e., $I_{\perp}$) is typically measured. The denominator represents the total intensity of light in the three-dimensional space.

Beam-light polarization is defined as follows:[65]

$$P = \frac{I_{max} - I_{min}}{I_{max} + I_{min}} \tag{23}$$

where I_{max} is the intensity of light polarized in the direction which corresponds to maximum intensity; I_{min} is the intensity of light in the direction perpendicular to the first one. The denominator also represents the total intensity of light but in two-dimensional space. eq 23 is sometimes written using $I_{\parallel}$ instead of I_{max} and $I_{\perp}$ instead of I_{min}:[64]

$$P = \frac{I_{\parallel} - I_{\perp}}{I_{\parallel} + I_{\perp}} \tag{24}$$

which is legitimate provided that we understand that P describes a two-dimensional case due to the missing factor of 2 in the denominator.

Formally, anisotropy and polarization calculated with eq 22 and eq 24, respectively, are closely related and interconvertible with[64]

$$r = \frac{2P}{3 - P} \tag{25}$$

Anisotropy has been proven to be an additive signal:[66]

$$r = r_L\frac{L}{L_0} + r_C\frac{C}{L_0} \tag{26}$$

and thus can be used to correctly calculate R with eq 8 and, then, build an accurate binding isotherm and accurately determine K_d with eq 11.[67] However, by combining the interconversion formula (eq 25) and the proof of anisotropy additivity (eq 26), we can easily conclude that P is non-additive (Note S4) and, thus, cannot be directly used to calculate R. The non-additivity of P (without transformations) was explained decades ago,[67,68] but it is still mistakenly used instead of r in eq 8 for finding R and K_d determination.

Additionally, some commercial instruments provide polarization (P) as a default output,[69,70] which can mislead users into calculating R based on P. Such a mistake can only be explained by a widely spread ignorance, as replacing P with r is not only correct but also does not require any changes in instrument hardware.

When one uses the non-additive P instead of additive r to calculate R with eq 8, the binding isotherm will slightly shift due to the systematic errors introduced to R (Figure 4). Without including any other source of systematic errors, these small shifts of binding isotherm cause <20% relative systematic error in $K_{d,det}$ for small $L_0/K_{d,true}$. However, the effect of this shift on the accuracy of $K_{d,det}$ grows with increasing $L_0/K_{d,true}$ and may result in >40% relative systematic errors for large $L_0/K_{d,true}$ (Figure 4B, Note S5 and Figure S1). The large discrepancy of $K_{d,det}$ from $K_{d,true}$ at high $L_0/K_{d,true}$ (Figure 4B, Figure S1) indicates that non-additive P should not be used to calculate R in K_d determination since the true value of $L_0/K_{d,true}$ is unknown *a priori*. If P is the default output of a commercial instrument,[24,25] it should be converted to r with interconversion formula (eq 25) before calculating R and conducting the standard downstream procedures of K_d determination, such as building binding isotherm and non-linear regression.

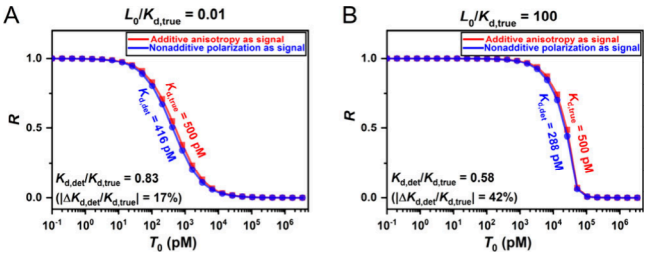

Figure 4. Comparison of the results produced by additive anisotropy (r) and non-additive polarization (P): binding isotherms and $K_{d,det}$ obtained with anisotropy (red) and polarization (blue) at $L_0/K_{d,true}$ = 0.01 (A) and $L_0/K_{d,true}$ = 100 (B). In the simulation, the theoretical/input $K_{d,true}$ = 500 pM.

3.2.1.3. Diffusivity-Based Methods. A signal from the ligand (used in eq 8) must change upon complex formation. The target−ligand complex is larger than unbound ligand and this size difference creates a foundation for size-dependent signals. A larger size results in slower translational movement leading to velocity as a signal (as discussed in section 3.2.1.1 above). A larger size leads to slower rotational depolarization resulting in anisotropy as a signal (as discussed in section 3.2.1.2 above). Furthermore, a larger size leads to slower diffusion and, accordingly, the apparent diffusion coefficient D_{app} of the ligand was suggested and used as a signal in K_d determination. One of the methods utilizing D_{app} is based on monitoring Taylor dispersion of the ligand molecule in a laminar pipe flow within a capillary filled with the target.[71−73] No inherent sources of inaccuracy have been reported for this approach so far. Here, we analyze D_{app} for additivity, required for its use as signal in eq 8 for calculation of R, and prove that D_{app} is non-additive.

Two geometrically different implementations of finding K_d via determination of the apparent diffusion coefficient (by monitoring Taylor dispersion) have been suggested:[71−73] one method utilizes a short plug of the equilibrium mixture of T and L, while the other uses a continuous flow of the equilibrium mixture. In each method, the apparent diffusion coefficient, D_{app}, is found by fitting the signal proportional to the corresponding function with D_{app} as an unknown parameter.[72,74] In this work, we will not compare these two implementations of determining D_{app}, but only analyze if D_{app} is additive.

There are four components in the equilibrium mixture: L (unbound ligand), T (unbound target), C (target−ligand complex), and one solvent. If D_{app} is additive, it must satisfy:

$$D_{app} = D_{app,L}\frac{L}{L_0} + D_{app,C}\frac{C}{L_0} \tag{27}$$

https://doi.org/10.1021/acschembio.4c00259
ACS Chem. Biol. 2024, 19, 1852−1867

where $D_{app,L}$ and $D_{app,C}$ are the apparent diffusion coefficients for pure ligand L and pure complex C, respectively, and D_{app} is the apparent diffusion coefficient of L (resulting from both the unbound and target-bound ligand) in the equilibrium mixture.

In the Supporting Information (Note S6 and Figure S2), we prove the non-additivity of D_{app} with mathematical derivations and numerical simulations. As shown in the results of simulations in Figure 5, employing the additivity assumption

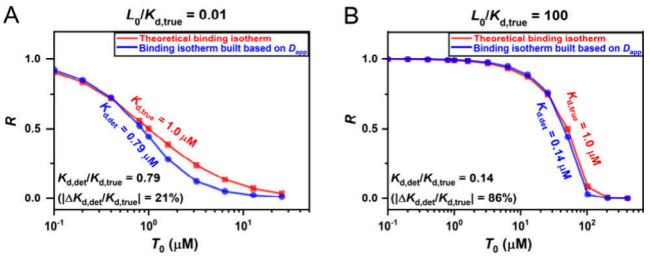

Figure 5. Comparison of the results produced by using apparent diffusion coefficient as signal (blue) and theoretical results (red) for $L_0/K_{d,true}$ = 0.01 (A) and $L_0/K_{d,true}$ = 100 (B). In the simulation, the theoretical/input $K_{d,true}$ = 1.0 μM.

of eq 27 results in large systematic errors in $K_{d,det}$, especially for high $L_0/K_{d,true}$ (Figure 5B). Consequently, we consider the diffusion coefficient, along with Taylor-dispersion methods, unsuitable for accurately determining K_d.

Although the apparent diffusion coefficient cannot be directly used to calculate R due to its non-additivity, R can be determined by analyzing an additive signal (e.g., fluorescence) that varies with the fraction of unbound ligand due to the differing diffusivities of L and C.[23] Species with different diffusion coefficients can undergo incomplete separation in laminar flow, a phenomenon known as transient incomplete separation (TIS).[75−77] Based on the theory of TIS, we developed the method of "accurate constant via transient incomplete separation" (ACTIS) using laser-induced fluorescence (LIF) or mass spectroscopy (MS) as detection methods.[23] ACTIS has been validated to be accurate, robust, and rugged both in computer simulations and with physical instruments.[78−80]

3.2.2. Mis-calibration of Signal-Detecting Instrument and Inaccurate Calibration Parameters. K_d determination relies on measuring signal changes due to complex formation. For accurate R values, the instrument detecting the ligand should be properly calibrated, ensuring a linear relationship between the detected signal and concentration. Mis-calibrated instruments can introduce systematic errors in R, affecting the accuracy of $K_{d,det}$. The necessity of appropriate calibration for signal-detecting instruments is well known, and calibration procedures vary from instrument to instrument.[81−83] In the Supporting Information (Note S7 and Figure S3), we demonstrate the effect of a mis-calibrated fluorescence detector on $K_{d,det}$.

Calibration parameters are often used in data analysis to standardize detected signals.[22,64,84] Accurate calibration parameters need to be determined prior to K_d-determination experiments. Errors in calibration parameters lead to errors in calculated R, impacting the accuracy of $K_{d,det}$. As an example, here we show the effect of errors in one common calibration parameter, φ (the quantum yield of target-bound ligand relative to that of unbound ligand in fluorescence detection), on the accuracy of $K_{d,det}$. Additionally, we discuss methods to enhance the accuracy of the calibration parameter φ.

In K_d-determination approaches detecting changes in fluorescence intensity due to the target's binding to the ligand (where the ligand denotes the component labeled with a fluorophore and of smaller size), fluorescence quenching (i.e., quantum yield change of a fluorophore) often occurs when the ligand binds to the target.[85] In complete-separation approaches, such as non-equilibrium capillary electrophoresis of equilibrium mixtures (NECEEM), R is calculated with eq 6 which involves a calibration parameter, φ, the quantum yield of the target-bound ligand relative to that of the unbound ligand.[22,31,32] Here, we compare $K_{d,det}$ to $K_{d,true}$ by introducing a 10% relative systematic error to φ (i.e., $\Delta\varphi/\varphi$ = 0.1) across a wide range of $L_0/K_{d,true}$ (Figure 6). The large relative

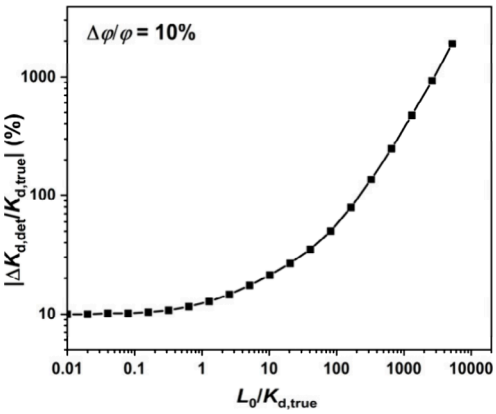

Figure 6. Dependence of relative systematic error of $K_{d,det}$ (i.e., |Δ$K_{d,det}/K_{d,true}$|) on $L_0/K_{d,true}$ with adding 10% relative systematic error in φ (i.e., $\Delta\varphi/\varphi$ = 10%) for a complete-separation approach with fluorescence as the signal.

systematic error in $K_{d,det}$ (|Δ$K_{d,det}/K_{d,true}$|) at high $L_0/K_{d,true}$ (as depicted in Figure 6) underscores the importance of accurately determining φ in complete-separation approaches.

In complete-separation approaches, φ is determined by comparing the signal area under the peak for pure complex (S_C*) to the area for pure ligand (S_L*):[22,31,32]

$$\varphi = \frac{S_C^*}{S_L^*} \tag{28}$$

Determining accurate φ necessitates finding S_L* and S_C* from pure ligand and pure complex, respectively, with identical concentrations, and accurately measuring the corresponding areas. To meet these requirements, we first need to decide on the concentration of ligand L_0 to use in order to produce S_L* in eq 28. While using the ligand concentration of L_0 = LOQ minimizes systematic errors in $K_{d,det}$ derived from systematic errors in L_0, T_0, and R,[17] we recommend employing a higher ligand concentration of $L_0 \geq 10 \times$ LOQ in the preliminary experiment to determine S_L*. A sample with higher ligand concentration (e.g., $L_0 = 10 \times$ LOQ) can yield a larger and more easily defined area of S_L* (and S_C*), leading to more accurate measured signal areas and reducing errors in determined φ.

To measure the area of S_C* from pure complex with the same concentration, i.e., L_0, the conditions outlined in eq 9 should be met to bind all ligands with a total concentration of L_0. To increase the likelihood of meeting the condition of T_0

https://doi.org/10.1021/acschembio.4c00259
ACS Chem. Biol. 2024, 19, 1852−1867

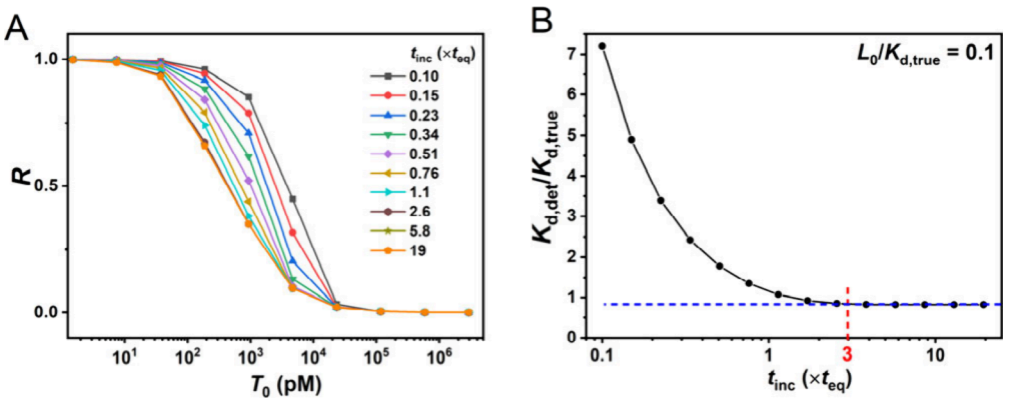

Figure 7. Dependencies of representative binding isotherms (A) and $K_{d,det}/K_{d,true}$ (B) on incubation time t_{inc}. In the simulations, $L_0/K_{d,true}$ was chosen to be 0.1. Due to the assumption of pseudo-first order conditions (either $T_0 \ll L_0$ and $L \approx L_0$ or $L_0 \ll T_0$ and $T \approx T_0$) satisfied by each EM, the stabilized $K_{d,det}$ was slightly smaller than the input $K_{d,true}$, i.e., stabilized $K_{d,det}/K_{d,true}$ was slightly smaller than unit, which does not affect estimating the sufficient incubation time.

$\gg K_{d,true}$ (unknown) (eq 9), the equilibrium mixture used for measuring S_C*, should contain the highest possible target concentration T_0, which is the solubility of the target in the sample buffer. Note that the increase in sample viscosity caused by high T_0 would unlikely affect the accuracy of measured S_C* in complete-separation approaches because signals (peak areas) are independent of viscosities. Furthermore, to ensure the condition of $T_0 > L_0$ (in eq 9) is met, L_0 used in determining S_L* and S_C* cannot be excessively high. Therefore, we recommend using L_0 = 10 × LOQ and T_0 = "solubility of target" as the component concentrations in the equilibrium mixture for measuring S_C*. It is important to emphasize that all conditions of preliminary experiments, e.g., temperature, sample buffer, detection system, etc., should be identical to those in the subsequent K_d-determination experiments to ensure the determined φ is a correct calibration parameter in downstream data analysis.

Unlike complete-separation approaches, incomplete-separation approaches, e.g., ACTIS, do not require the parameter φ to correct signal S_C* in eq 8 for calculating R, since the detected fluorescence intensity multiplied with a constant quenching coefficient satisfies the requirement of signal superposition (eq 7).[23] Thus, although fluorescence quenching affects the detected signal S, its presence does not affect the accuracy of $K_{d,det}$ obtained in approaches with incomplete separation of free ligand from the complex.

In the Supporting Information (Note S8), we also investigate the effect of the errors in another method-specific calibration parameter, G (grating factor in fluorescence anisotropy), on the accuracy of $K_{d,det}$ and provide suggestions on improving the accuracy of the experimentally determined G.

3.2.3. Not Reaching Equilibrium or Saturation. Careful and correct pre-experimental calculations and experimental design are crucial for the accurate determination of K_d. In these preparative steps, researchers should decide on (*i*) the most suitable K_d-determination approach for the studied binding pair, (*ii*) experimental conditions, such as temperature and wavelength of the light source, (*iii*) the concentration of each binding partner in each equilibrium mixture, and (*iv*) the incubation time for the samples, among other factors. Among these experimental parameters, the total concentrations of binding partners in equilibrium mixtures (i.e., L_0 and T_0) and the incubation time for the samples are usually difficult to choose due to the lack of reliable input information. Here we demonstrate the effect of insufficient incubation time and failure to reach saturation in the binding isotherm (caused by the mis-selection of concentrations) on the accuracy of $K_{d,det}$. We provide suggestions on how to ensure the incubation time is sufficient and how to ensure that the equilibrium mixture with the highest T_0 satisfies the saturation condition.

3.2.3.1. Not Reaching Equilibrium in the Binding Process. The first experimental step of the classic methodology of K_d determination is to prepare a set of equilibrium mixtures containing a constant concentration of the limiting component L_0 and varied concentrations T_0 of the target. To minimize the systematic error in $K_{d,det}$ propagated from ΔL_0, ΔT_0, and ΔR, we should choose L_0 = LOQ.[17] In practice, the lowest nonzero T_0 is usually chosen as low as possible (often much lower than L_0),[16] for which the pseudo-first-order conditions of $T_0 \ll L_0$ and $L \approx L_0$ are satisfied. Therefore, the characteristic time t_{eq} (eq 18) of the reversible binding process (eq 2) with the lowest nonzero T_0 is expressed as

$$t_{eq} \approx (k_{off} + k_{on}L_0)^{-1} \quad \text{or}$$
$$t_{eq} \approx (k_{off} + k_{on}\text{LOQ})^{-1} \quad \text{when } L_0 = \text{LOQ} \tag{29}$$

which limits (represents the longest) characteristic time for all the binding processes with different T_0 in a single K_d-determination experiment. To reach ≥95% of the equilibrium concentration of the complex with the lowest nonzero T_0, the incubation time (t_{inc}) must reach at least 3 times t_{eq} shown in eq 29 (Note S9). In studies of molecular pairs with high affinity (i.e., low K_d with high k_{on} and/or low k_{off}) and using low L_0 in all samples, the sufficient incubation time (i.e., $t_{inc} \geq 3t_{eq}$) can be extremely long (e.g., a few days) (Note S9). Thus, it is common to overestimate $K_{d,det}$ due to using insufficient incubation time.[14]

To demonstrate the effect of insufficient incubation time on the accuracy of $K_{d,det}$, we simulated the binding isotherms using the spreadsheet Data S1. We utilized the incubation time within a range of 0.1t_{eq} to 19t_{eq} (t_{eq} was calculated using eq 29) with a 1.5-fold step size, using $L_0/K_{d,true}$ = 0.1 (Figure 7A), and summarized the dependence of $K_{d,det}/K_{d,true}$ on the incubation time (Figure 7B). The results of the simulations (Figure 7B) show that, even with low $L_0/K_{d,true}$ = 0.1, insufficient incubation time can cause $K_{d,det}$ to be several times higher

https://doi.org/10.1021/acschembio.4c00259
ACS Chem. Biol. 2024, 19, 1852−1867

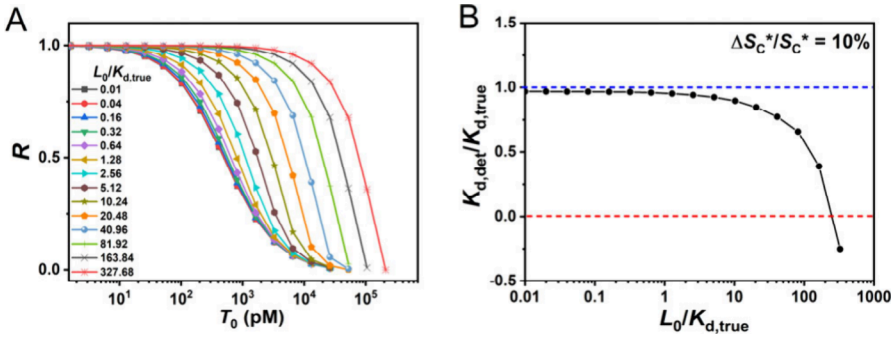

Figure 8. Dependencies of representative binding isotherms (A) and $K_{d,det}/K_{d,true}$ (B) on $L_0/K_{d,true}$ with adding 10% relative systematic error in S_C^*, i.e., the measured S_C^* is 10% higher than true S_C^* determined at saturation. In these simulations, we assume the cumulative signal S decreases with the increase of T_0.

than $K_{d,true}$. As expected, both the binding isotherm and $K_{d,det}$ stabilize when $t_{inc} \geq 3t_{eq}$.

Although there are some experimental and mathematical approaches to estimate sufficient incubation time (Note S10), at this stage, the only reliable method of eliminating the effect of incubation time on the accuracy of $K_{d,det}$ is conducting multiple K_d-determination experiments with increased incubation times until $K_{d,det}$ stabilizes.[14] Note that, as equilibration time is longer at lower T_0, one can plan a sequence of experiments so that equilibrium mixtures with higher T_0 are analyzed before equilibrium mixtures with lower T_0 allowing the latter more time for equilibration.

3.2.3.2. Not Reaching Saturation in Binding Isotherm. For K_d-determination approaches with complete separation of unbound ligand from target-bound ligand, although a complete binding isotherm with R ranging from 0 to 1 is preferable, a partial binding isotherm can be used to determine K_d if the quantum yield ratio φ is accurately predetermined (eq 28). However, in most K_d-determination approaches, free ligand and complex cannot be completely separated, and R is calculated with eq 8, in which the signals from pure ligand and pure complex (i.e., S_L^* and S_C^*) play crucial roles. As we mentioned above, the measurement of S_L^* is trivial, while the determination of S_C^* requires that the binding process reach saturation, i.e., $C \gg L$. Since all the R values are calculated based on S_L^* and S_C^* (eq 8), an inaccurate S_C^*, resulting from a binding isotherm not reaching saturation, can distort the whole binding isotherm and significantly reduce the accuracy of $K_{d,det}$.

Here, we simulated binding isotherms (with Data S1) by adding 10% relative systematic error in S_C^* (i.e., binding isotherm does not reach saturation and $\Delta S_C^*/S_C^* = 0.1$) for a large range of $L_0/K_{d,true}$ (Figure 8A), and summarized the dependence of the $K_{d,det}/K_{d,true}$ ratio on $L_0/K_{d,true}$ (Figure 8B). Figure 8B indicates that, for binding isotherms not reaching saturation conditions, $K_{d,det}$ can be much lower than the true K_d (even reaching impossible negative values) at high $L_0/K_{d,true}$, emphasizing the importance of using T_0 that allows the binding isotherm to reach saturation condition.

To ensure that the binding isotherm reaches saturation, the conditions of the equilibrium mixture with the highest T_0 should satisfy eq 9, i.e., $T_0 > L_0$ and $T_0 \gg K_{d,true}$. The condition of $T_0 > L_0$ is easy to satisfy if L_0 is chosen to be close to the LOQ of the instrument (usually in the pico- to nanomolar range). However, it is difficult to conclude if the condition $T_0 \gg K_{d,true}$ is satisfied without knowing the true K_d.

A potential solution to this problem is to use the largest possible target concentration T_0 (which represents the solubility of the target in the sample buffer), in the equilibrium mixture (as discussed in section 3.2.2. for determining φ in complete-separation approaches). However, this solution has two main limitations for incomplete-separation approaches. First, using excessively high T_0 itself may affect the accuracy of measured S_C^*. For instance, the increased viscosity of the sample caused by high T_0 (e.g., protein concentration) can affect the detected signals for diffusivity-based (or -related) approaches such as ACTIS and MST. Second, if the binding isotherm reaches saturation with T_0 much smaller than solubility, reaching the highest possible T_0 would waste a large amount of the target, which is often a precious protein.

Therefore, to ensure that a binding isotherm reaches saturation and to avoid the drawbacks associated with using excessively high T_0, here we suggest a criterion for saturation in a binding isotherm. The criterion entails ensuring that zero lies within the uncertainty range of the slope for the linear fitting of the "cumulative signal S versus T_0" obtained from the equilibrium mixtures with the three highest T_0. Additionally, the highest T_0 should be at least 2-fold greater than the lowest T_0 in the three equilibrium mixtures.

3.2.4. Estimating Systematic Error in R Quantitatively. To provide researchers a comprehensive guidance to minimize the systematic error in R, we summarize the measures discussed above into a checklist, which is an expanded version of the checklist proposed by Jarmoskaite et al. (see Table S1).[14] By using the checklist in Table S1, researchers can reduce the likelihood of common theoretical or experimental mistakes in determining R and thus significantly reduce ΔR. Based on the experimentalist's confidence in the determined calibration parameters, the accuracy of the instruments used to measure signals, and other factors, the range of minimized $\Delta R/R$ (relative systematic error of R) with a certain confidence level might be estimated. However, at this stage, we have not identified an approach for quantitatively determining the interval of minimized systematic error of R that can be used as a reliable input to calculate the systematic error range of $K_{d,det}$. Note that, the random error of R (δR) is independent to ΔR and is translated into the random error of $K_{d,det}$ (σ) through nonlinear regression of a binding isotherm.

3.3. Sources and Confidence Intervals of Systematic Errors in Concentrations. Sources of systematic errors in T_0 and L_0 arise from various factors. If concentrations are calculated based on the weight of solid material and volume of solvent, imperfectly calibrated mass- and volume-measuring

https://doi.org/10.1021/acschembio.4c00259
ACS Chem. Biol. 2024, 19, 1852−1867

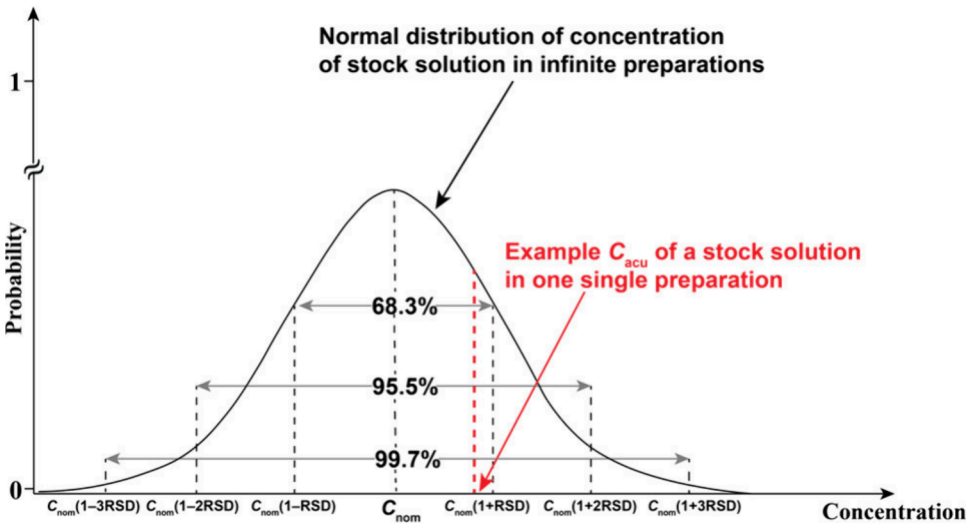

Figure 9. Demonstration of the relationship between the accurate concentration (C_{acu}) of a stock solution in one single preparation and the concentration distribution in an infinite number of preparations. With minimized systematic error in concentration, we assume the average concentration is equal to the nominal concentration C_{nom}.

equipment as well as errors in product purity, can lead to systematic errors in concentrations. If concentrations are calculated using spectrophotometry (Lambert−Beer law), systematic errors in molar extinction coefficients will result in systematic errors in concentrations. These common sources can induce systematic errors in target and ligand concentrations of stock solutions, which, in turn, can propagate into systematic errors in concentrations of other diluted solutions used in K_d-determination experiments. Another common source of systematic errors in T_0 and L_0 occurring at any step of an experiment is solute adsorption onto pipet tips, vials, channels, etc. In the Supporting Information, we illustrate the effect of systematic errors in T_0 and L_0 on the accuracy of $K_{d,det}$ for a large range of L_0/K_d (Figure S5) and delve into the common sources of systematic errors in concentrations along with strategies to mitigate them (Note S11). To assist researchers in minimizing systematic error in concentrations L_0 and T_0, the measures to minimize ΔL_0 and ΔT_0 are summarized in a checklist (Table S1) in the Supporting Information.

When the systematic errors of variables are minimized, it is important to have an approach that can quantitatively assess the minimized systematic errors since estimating the systematic error in $K_{d,det}$ from a single binding isotherm using error-propagation methods requires input values for ΔL_0, ΔT_0, and ΔR.[18,26−28] If exact values of systematic errors in variables can be determined, then the case is trivial as the variable can be simply corrected for this systematic error. Conversely, if nothing is known about systematic errors in variables, then the problem is ill-posed as completely unknown systematic errors cannot be propagated. However, there is a third case where the exact values of systematic errors in variables are unknown, but the confidence intervals of the systematic errors with desired confidence levels can be quantitatively assessed. Confidence intervals of systematic errors are not commonly discussed in statistics, but they likely play a crucial role in the determination of physicochemical parameters with nonlinear regression. Here, we discuss two cases of assessing confidence intervals of systematic errors in concentrations.

The first case involves a rough estimation based on experiences, akin to the estimation of $\Delta R/R$ range mentioned in section 3.2.4. If techniques listed in Table S1 (e.g., SDS-PAGE) for determining large systematic errors or approaches of method optimization (e.g., surface-modification) are inaccessible, an experienced experimentalist should be able to estimate the maximum ranges of relative systematic errors in concentrations with some confidence, e.g., ± 20% for ligand concentration and ±30% for target concentration with confidence.

The second case involves a quantitative assessment based on the relative random errors (i.e., relative standard deviations, RSD) in concentrations of stock solutions. If all necessary procedures for minimizing systematic errors (e.g., device calibration, purity measurement, and method optimization) have been properly conducted, we can reasonably assume that the systematic errors in L_0 and T_0 of equilibrium mixtures are from the random errors in the concentrations of ligand and target stock solutions, i.e., the normally distributed concentrations of stock solutions in infinite preparations (Figure 9). This assumption is valid because all the diluted solutions used in K_d determination with nonlinear regression are prepared from a single condensed ligand stock solution and a single condensed target stock solution. The random errors in the concentrations of stock solutions (present in an infinite number of sample preparations) are usually much greater than those of equilibrium mixtures due to the more complicated preparation procedure with more error sources. Thus, the confidence intervals of systematic errors in L_0 and T_0 (in equilibrium mixtures) can be estimated by measuring the RSD of the concentrations of their stock solutions in multiple preparations. Since there is no reliable measure to determine concentration directly, RSD of concentrations should be determined by experimentally measuring the spectroscopic signals (e.g., light absorption or fluorescence intensity) from stock solutions in multiple preparations (see an example in Table S2).

For a single preparation of stock solution with a nominal (desired) concentration C_{nom}, the confidence interval (e.g., with 68.3% confidence level) of systematic error can be calculated as $\Delta C \in [-C_{nom} \times RSD, C_{nom} \times RSD]$, for which the confidence interval of accurate concentration C_{acu} is $C_{acu} \in [C_{nom}(1 - RSD), C_{nom}(1 + RSD)]$ (Figure 9). Note that, the

https://doi.org/10.1021/acschembio.4c00259
ACS Chem. Biol. 2024, 19, 1852−1867

confidence level of systematic error or accurate concentration can be varied by using different numbers of RSD in the calculation of confidence intervals. As a result, due to equilibrium mixtures being prepared by diluting stock solutions, the confidence intervals (e.g., with 68.3% confidence level) of systematic errors in nominal L_0 and T_0 can be assessed as $\Delta L_0 \in [-\text{RSD} \times L_0, \text{RSD} \times L_0]$ and $\Delta T_0 \in [-\text{RSD} \times T_0, \text{RSD} \times T_0]$, respectively. It is important to emphasize that the confidence intervals of ΔL_0 and ΔT_0 derived from the RSD of concentrations of stock solutions are the lower limits of systematic error ranges assuming that all other systematic errors in the concentrations of stock solutions have been eliminated. Despite lacking an approach for quantitatively assessing the confidence interval of ΔR, the approach of finding the lower limits of confidence intervals of ΔL_0 and ΔT_0 explained here will make the existing numerical statistical methods of calculating the confidence interval of $K_{d,true}$ more comprehensive and practical for molecular scientists.[26−28]

4. CONCLUDING REMARKS

Since the systematic error in a determined K_d ($\Delta K_{d,det}$) is translated from the systematic errors in the variables used to determine K_d, i.e., ΔL_0, ΔT_0, and ΔR (Figure 1B), understanding the sources of systematic errors in all variables and minimizing these errors are pivotal to minimizing $\Delta K_{d,det}$. It is crucial to emphasize that systematic errors in the variables can result in an incorrect ranking of ligands during high-throughput screening. This challenges the common belief that such errors systematically shift all $K_{d,det}$ values in the same direction without affecting the ranking order. For instance, ligands with low true K_d values can have high $L_0/K_{d,true}$ values; without minimizing the systematic errors in variables, $K_{d,det}$ can be much greater than $K_{d,true}$, wrongly categorizing these ligands as low-potency.

To determine an accurate K_d, the first step is to ensure there is no theoretical or experimental mistake in the K_d-determination approach. Such mistakes can introduce systematic errors in R, and eventually translate into systematic errors in $K_{d,det}$, which can be extremely large at unfavorable (large) values of $L_0/K_{d,true}$ (see, for example, Figure 3). In this work, we discussed the most common sources of systematic errors in R, such as non-additive signals, mis-calibrated instruments, inaccurate calibration parameters, etc., and quantitatively studied the effect of errors from these sources on the accuracy of $K_{d,det}$. We also provided suggestions on how to reduce or eliminate the systematic error in R caused by the common error sources. With careful theoretical and experimental design and proper instrument calibration, ΔR can be minimized, while the confidence interval of the minimized ΔR cannot be quantitatively determined at this stage.

The sources of systematic errors in concentrations (i.e., ΔL_0, ΔT_0), such as mis-calibrated measuring equipment, product impurities, and reagent adsorption onto surfaces, have been well-studied, and many approaches to eliminate these error sources have been developed (Note S11).[86−89] In this work, we summarized the measures of eliminating or minimizing ΔR, ΔL_0, and ΔT_0 caused by the common error sources into a checklist (Table S1), which is a convenient tool for researchers in the field of K_d determination. For any specific K_d-determination approach, researchers should establish a standard operating procedure (SOP) for minimizing systematic errors in concentrations based on the chemical properties of the ligand and target used. The SOP should be established prior to any experiment, and it should be strictly followed during the K_d-determination experiments.

Although the systematic errors in concentrations cannot be fully eliminated, and their true values can hardly be determined accurately, the confidence intervals of the minimized systematic errors in concentrations can be quantitatively assessed with the quantitative study of random errors in concentrations of stock solutions. By combining the quantitatively assessed confidence intervals of systematic errors in concentrations with the existing numerical statistical methods, the lower limit of confidence interval of $K_{d,true}$ can be determined.[26−28] In addition, these confidence intervals are being instrumental in the ongoing development of a new highly practical tool for assessment of the accuracy confidence interval of $K_{d,true}$.[18]

In summary, in this work, we theoretically analyze the common sources of systematic errors in K_d determination. Our findings offer valuable insights and practical strategies that are crucial for researchers aiming to maximize the accuracy of K_d measurements in binding studies. By thoroughly understanding and addressing these error sources, this work provides a robust framework that can be integrated into both academic curricula and professional practice, thereby enhancing the reliability of experimental outcomes. Additionally, our study serves as a critical reference for peer reviewers and journal editors in assessing the methodological soundness of research articles reporting K_d values. Ultimately, the adoption of these guidelines will foster higher standards of reliability in the field, benefiting the wider scientific community and advancing the quality of research in molecular interactions.

■ ASSOCIATED CONTENT

Data Availability Statement

Additional supplementary files can be found on Figshare (DOI: 10.6084/m9.figshare.25464685): Figures.zip, figures from the main text and Supporting Information (Origin, Adobe Illustrator, PNG, and TIFF files); Data S1.xlsx, spreadsheet for simulating binding isotherms (Excel file); Checklist.pdf, checklist for minimizing the systematic errors of variables in K_d determination with nonlinear regression (PDF file).

Supporting Information

The Supporting Information is available free of charge at https://pubs.acs.org/doi/10.1021/acschembio.4c00259.

Theory developments, derivations of equations, mathematical proofs, results of simulations, checklist for eliminating error sources, experimental considerations, and experimental results (PDF)

■ AUTHOR INFORMATION

Corresponding Author

Sergey N. Krylov − *Department of Chemistry, York University, Toronto, Ontario M3J 1P3, Canada; Centre for Research on Biomolecular Interactions, York University, Toronto, Ontario M3J 1P3, Canada;* orcid.org/0000-0003-3270-2130; Email: skrylov@yorku.ca

Authors

Tong Ye Wang − *Department of Chemistry, York University, Toronto, Ontario M3J 1P3, Canada; Centre for Research on Biomolecular Interactions, York University, Toronto, Ontario M3J 1P3, Canada;* orcid.org/0000-0001-9462-7194

https://doi.org/10.1021/acschembio.4c00259
ACS Chem. Biol. 2024, 19, 1852−1867

Jean-Luc Rukundo − *Department of Chemistry, York University, Toronto, Ontario M3J 1P3, Canada; Centre for Research on Biomolecular Interactions, York University, Toronto, Ontario M3J 1P3, Canada;* orcid.org/0000-0003-3626-2515

Zhiyuan Mao − *Department of Chemistry, York University, Toronto, Ontario M3J 1P3, Canada; Centre for Research on Biomolecular Interactions, York University, Toronto, Ontario M3J 1P3, Canada*

Complete contact information is available at: https://pubs.acs.org/10.1021/acschembio.4c00259

Notes

The authors declare no competing financial interest.

■ ACKNOWLEDGMENTS

This work was supported by funds from York University towards the Catalyzing Interdisciplinary Research Cluster "Technologies for Identification and Control of Infectious Diseases".

■ SYMBOLS

K_d, equilibrium dissociation constant
$K_{d,det}$, (experimentally) determined value of K_d
$K_{d,true}$, (unknown) true value of K_d
$\Delta K_{d,det}$, systematic error of $K_{d,det}$
L_0, total concentration of the ligand
L, equilibrium concentration of the ligand
ΔL_0, systematic error of L_0
T_0, total concentration of the target
T, equilibrium concentration of the target
ΔT_0, systematic error of T_0
C, equilibrium concentration of the target−ligand complex
R, fraction of unbound ligand in the equilibrium mixture of ligand and target
ΔR, systematic error of R
δR, random error of R
σ, standard deviation (uncertainty) of $K_{d,det}$ obtained with nonlinear regression
RSD, relative standard deviation
LOQ, limit of quantitation of the instrument used to detect the ligand
k_{on}, rate constant of complex formation
k_{off}, rate constant of complex dissociation
S_L, signal from the unbound ligand
S_C, signal from the target−ligand complex
S, cumulative signal from the unbound ligand and the target-bound ligand in the equilibrium mixture
S_L*, signal from pure ligand with a concentration of L_0
S_C*, signal from pure complex with a concentration of L_0
φ, factor by which the signal of ligand changes when it binds the target
t_{eq}, characteristic equilibration time under the condition of pseudoequilibrium in the binding process
t_{sep}, characteristic separation time
t_{inc}, incubation time of a mixture of ligand and target
r, anisotropy, or the cumulative anisotropy determined from the equilibrium mixture
$I_{\parallel}$, intensity of light emitted by a fluorophore with a polarization orientation parallel to that of the excitation light
$I_{\perp}$, intensity of emitted light with a polarization orientation perpendicular to that of the excitation light
I_{max}, intensity the of light polarized in the direction that corresponds to maximum intensity
I_{min}, intensity of light polarized in the direction that corresponds to minimum intensity
P, polarization, or the cumulative polarization measured from the equilibrium mixture
D_{app}, apparent diffusion coefficient determined from the equilibrium mixture
G, grating factor in fluorescence anisotropy
C_{nom}, nominal (experimentally desired) concentration
C_{acu}, accurate (true) concentration
ΔC, systematic error of concentration

■ REFERENCES

(1) Kenakin, T.; Williams, M. Defining and characterizing drug/compound function. *Biochem. Pharmacol.* **2014**, *87* (1), 40−63.
(2) Petrauskas, V.; Kazlauskas, E.; Gedgaudas, M.; Baranauskienė, L.; Zubrienė, A.; Matulis, D. Thermal shift assay for protein-ligand dissociation constant determination. *TrAC, Trends Anal. Chem.* **2024**, *170*, 117417.
(3) Dahl, G.; Akerud, T. Pharmacokinetics and the drug-target residence time concept. *Drug Discovery Today* **2013**, *18* (15−16), 697−707.
(4) Chock, P. B.; Rhee, S. G.; Stadtman, E. R. Interconvertible enzyme cascades in cellular regulation. *Annu. Rev. Biochem.* **1980**, *49* (1), 813−841.
(5) Miles, L.; Plow, E. Plasminogen receptors: ubiquitous sites for cellular regulation of fibrinolysis. *Fibrinolysis* **1988**, *2* (2), 61−71.
(6) Bottari, F.; Daems, E.; de Vries, A.-M.; Van Wielendaele, P.; Trashin, S.; Blust, R.; Sobott, F.; Madder, A.; Martins, J. C.; De Wael, K. Do aptamers always bind? The need for a multifaceted analytical approach when demonstrating binding affinity between aptamer and low molecular weight compounds. *J. Am. Chem. Soc.* **2020**, *142* (46), 19622−19630.
(7) Fielding, L. NMR methods for the determination of protein-ligand dissociation constants. *Prog. Nucl. Magn. Reson. Spectrosc.* **2007**, *51* (4), 219−242.
(8) Hoare, S. R.; Fleck, B. A.; Williams, J. P.; Grigoriadis, D. E. The importance of target binding kinetics for measuring target binding affinity in drug discovery: a case study from a CRF1 receptor antagonist program. *Drug Discovery Today* **2020**, *25* (1), 7−14.
(9) Archakov, A. I.; Govorun, V. M.; Dubanov, A. V.; Ivanov, Y. D.; Veselovsky, A. V.; Lewi, P.; Janssen, P. Protein-protein interactions as a target for drugs in proteomics. *Proteomics* **2003**, *3* (4), 380−391.
(10) Strange, P. G. Antipsychotic drugs: importance of dopamine receptors for mechanisms of therapeutic actions and side effects. *Pharmacol. Rev.* **2001**, *53* (1), 119−133.
(11) Tracy, T. S.; Hummel, M. A. Modeling kinetic data from in vitro drug metabolism enzyme experiments. *Drug Metab. Rev.* **2004**, *36* (2), 231−242.
(12) Halford, S. E. An end to 40 years of mistakes in DNA-protein association kinetics? *Biochem. Soc. Trans.* **2009**, *37* (2), 343−348.
(13) Sims, R. J.; Reinberg, D. Histone H3 Lys 4 methylation: caught in a bind? *Genes Dev.* **2006**, *20* (20), 2779−2786.
(14) Jarmoskaite, I.; AlSadhan, I.; Vaidyanathan, P. P.; Herschlag, D. How to measure and evaluate binding affinities. *Elife* **2020**, *9*, No. e57264.
(15) Pollard, T. D. A guide to simple and informative binding assays. *Mol. Biol. Cell* **2010**, *21* (23), 4061−4067.
(16) Hulme, E. C.; Trevethick, M. A. Ligand binding assays at equilibrium: validation and interpretation. *Br. J. Pharmacol.* **2010**, *161* (6), 1219−1237.
(17) Wang, T. Y.; Ji, H.; Everton, D.; Le, A. T.; Krylova, S. M.; Fournier, R.; Krylov, S. N. Fundamental Determinants of the Accuracy of Equilibrium Constants for Affinity Complexes. *Anal. Chem.* **2023**, *95* (42), 15826−15832.
(18) Wang, T.; Latimer, J.; Rukundo, J. L.; Kogan, I.; Krylova, S.; Schreiber, S.; Kohlmann, P.; Jose, J.; Krylov, S. Introducing

Quantitative Assessment of Accuracy for the Equilibrium Constant of Affinity Complexes. *ChemRxiv Preprint* **2024**, chemrxiv-2024-lg58f.
(19) Krylov, S. N. Underestimation of the Complexity of Kd Determination: Causes, Implications, and Ways to Improve. *ACS Meas. Sci. Au* **2024**, *4* (3), 231−232.
(20) Fielding, L. NMR methods for the determination of protein-ligand dissociation constants. *Curr. Top. Med. Chem.* **2003**, *3* (1), 39−53.
(21) Jerabek-Willemsen, M.; Wienken, C. J.; Braun, D.; Baaske, P.; Duhr, S. Molecular interaction studies using microscale thermophoresis. *Assay Drug Dev. Technol.* **2011**, *9* (4), 342−353.
(22) Kanoatov, M.; Galievsky, V. A.; Krylova, S. M.; Cherney, L. T.; Jankowski, H. K.; Krylov, S. N. Using nonequilibrium capillary electrophoresis of equilibrium mixtures (NECEEM) for simultaneous determination of concentration and equilibrium constant. *Anal. Chem.* **2015**, *87* (5), 3099−3106.
(23) Sisavath, N.; Rukundo, J. L.; Le Blanc, J. Y.; Galievsky, V. A.; Bao, J.; Kochmann, S.; Stasheuski, A. S.; Krylov, S. N. Transient incomplete separation facilitates finding accurate equilibrium dissociation constant of protein-small molecule complex. *Angew. Chem.* **2019**, *131* (20), 6707−6711.
(24) Rusling, J. F. Computerized method for mechanistic classification of one-electron potentiostatic current-potential curves. *Anal. Chem.* **1983**, *55* (11), 1713−1718.
(25) Johnson, M. L.; Correia, J. J.; Yphantis, D. A.; Halvorson, H. R. Analysis of data from the analytical ultracentrifuge by nonlinear least-squares techniques. *Biophys. J.* **1981**, *36* (3), 575−588.
(26) Kazmierczak, N. P.; Chew, J. A.; Vander Griend, D. A. Bootstrap methods for quantifying the uncertainty of binding constants in the hard modeling of spectrophotometric titration data. *Anal. Chim. Acta* **2022**, *1227*, 339834.
(27) Nguyen, T. H.; Rustenburg, A. S.; Krimmer, S. G.; Zhang, H.; Clark, J. D.; Novick, P. A.; Branson, K.; Pande, V. S.; Chodera, J. D.; Minh, D. D. Bayesian analysis of isothermal titration calorimetry for binding thermodynamics. *PLoS One* **2018**, *13* (9), No. e0203224.
(28) Feng, F.; Kepler, T. B. Bayesian estimation of the active concentration and affinity constants using surface plasmon resonance technology. *PloS one* **2015**, *10* (6), No. e0130812.
(29) Wells, J. A. Binding in the growth hormone receptor complex. *Proc. Natl. Acad. Sci. U. S. A.* **1996**, *93* (1), 1−6.
(30) Levengood, J. D.; Tolbert, B. S. Idiosyncrasies of hnRNP A1-RNA recognition: Can binding mode influence function. In *Seminars in cell & developmental biology*; Elsevier, 2019; Vol. *86*, pp 150−161.
(31) Teclemichael, E.; Le, A. T.; Krylova, S. M.; Wang, T. Y.; Krylov, S. N. Bulk Affinity Assays in Aptamer Selection: Challenges, Theory, and Workflow. *Anal. Chem.* **2022**, *94* (44), 15183−15188.
(32) Le, A. T.; Krylova, S. M.; Krylov, S. N. Determination of the Equilibrium Constant and Rate Constant of Protein-Oligonucleotide Complex Dissociation under the Conditions of Ideal-Filter Capillary Electrophoresis. *Anal. Chem.* **2019**, *91* (13), 8532−8539.
(33) Williamson, M. P. Using chemical shift perturbation to characterise ligand binding. *Prog. Nucl. Magn. Reson. Spectrosc.* **2013**, *73*, 1−16.
(34) Piñeiro, L.; Novo, M.; Al-Soufi, W. Fluorescence emission of pyrene in surfactant solutions. *Adv. Colloid Interface Sci.* **2015**, *215*, 1−12.
(35) Zhao, Q.; Tao, J.; Feng, W.; Uppal, J. S.; Peng, H.; Le, X. C. Aptamer binding assays and molecular interaction studies using fluorescence anisotropy-a review. *Anal. Chim. Acta* **2020**, *1125*, 267−278.
(36) Krylova, S. M.; Dove, P. M.; Kanoatov, M.; Krylov, S. N. Slow-dissociation and slow-recombination assumptions in nonequilibrium capillary electrophoresis of equilibrium mixtures. *Anal. Chem.* **2011**, *83* (19), 7582−7585.
(37) Berezovski, M.; Krylov, S. N. Nonequilibrium capillary electrophoresis of equilibrium mixtures- a single experiment reveals equilibrium and kinetic parameters of protein- DNA interactions. *J. Am. Chem. Soc.* **2002**, *124* (46), 13674−13675.
(38) Okhonin, V.; Berezovski, M. V.; Krylov, S. N. MASKE: Macroscopic approach to studying kinetics at equilibrium. *J. Am. Chem. Soc.* **2010**, *132* (20), 7062−7068.
(39) Chalmers, M. J.; Busby, S. A.; Pascal, B. D.; West, G. M.; Griffin, P. R. Differential hydrogen/deuterium exchange mass spectrometry analysis of protein-ligand interactions. *Expert Rev. Proteomics* **2011**, *8* (1), 43−59.
(40) Kanoatov, M.; Mehrabanfar, S.; Krylov, S. N. Systematic approach to optimization of experimental conditions in non-equilibrium capillary electrophoresis of equilibrium mixtures. *Anal. Chem.* **2016**, *88* (18), 9300−9308.
(41) Poole, S. K.; Patel, S.; Dehring, K.; Workman, H.; Poole, C. F. Determination of acid dissociation constants by capillary electrophoresis. *J. Chromatogr. A* **2004**, *1037* (1−2), 445−454.
(42) Pesce, A. J.; Michael, J. G. Artifacts and limitations of enzyme immunoassay. *J. Immunol. Methods* **1992**, *150* (1−2), 111−119.
(43) Nistor, C.; Emnéus, J. Immunoassay: potentials and limitations. *Compr. Anal. Chem.* **2005**, *44*, 375−427.
(44) Tighe, P. J.; Ryder, R. R.; Todd, I.; Fairclough, L. C. ELISA in the multiplex era: potentials and pitfalls. *PROTEOM. Clin. Appl.* **2015**, *9* (3−4), 406−422.
(45) Nguyen, B.; Tanious, F. A.; Wilson, W. D. Biosensor-surface plasmon resonance: quantitative analysis of small molecule-nucleic acid interactions. *Methods* **2007**, *42* (2), 150−161.
(46) Unser, S.; Bruzas, I.; He, J.; Sagle, L. Localized surface plasmon resonance biosensing: current challenges and approaches. *Sensors* **2015**, *15* (7), 15684−15716.
(47) Homola, J. Present and future of surface plasmon resonance biosensors. *Anal. Bioanal. Chem.* **2003**, *377*, 528−539.
(48) Petersen, R. L. Strategies using bio-layer interferometry biosensor technology for vaccine research and development. *Biosensors* **2017**, *7* (4), 49.
(49) Renaud, J.-P.; Chung, C.-w.; Danielson, U. H.; Egner, U.; Hennig, M.; Hubbard, R. E.; Nar, H. Biophysics in drug discovery: impact, challenges and opportunities. *Nat. Rev. Drug Discovery* **2016**, *15* (10), 679−698.
(50) Jug, A.; Bratkovič, T.; Ilaš, J. Biolayer interferometry and its applications in drug discovery and development. *TrAC, Trends Anal. Chem.* **2024**, *176*, 117741.
(51) Lee, N.; Wiegand, S. Thermophoretic micron-scale devices: practical approach and review. *Entropy* **2020**, *22* (9), 950.
(52) Magnez, R.; Bailly, C.; Thuru, X. Microscale thermophoresis as a tool to study protein interactions and their implication in human diseases. *Int. J. Mol. Sci.* **2022**, *23* (14), 7672.
(53) Asmari, M.; Michalcová, L.; Ibrahim, A. E.; Glatz, Z.; Wätzig, H.; El Deeb, S. Studying molecular interactions via capillary electrophoresis and microscale thermophoresis: A review. *Electrophoresis* **2023**, *44* (13−14), 1114−1142.
(54) Ward, W. H.; Holdgate, G. A. 7 Isothermal Titration Calorimetry in Drug Discovery. *Prog. Med. Chem.* **2001**, *38*, 309−376.
(55) Leavitt, S.; Freire, E. Direct measurement of protein binding energetics by isothermal titration calorimetry. *Curr. Opin. Struct. Biol.* **2001**, *11* (5), 560−566.
(56) Prozeller, D.; Morsbach, S.; Landfester, K. Isothermal titration calorimetry as a complementary method for investigating nanoparticle-protein interactions. *Nanoscale* **2019**, *11* (41), 19265−19273.
(57) Dalvit, C.; Gmür, I.; Rößler, P.; Gossert, A. D. Affinity measurement of strong ligands with NMR spectroscopy: Limitations and ways to overcome them. *Prog. Nucl. Magn. Reson. Spectrosc.* **2023**, *138−139*, 52−69.
(58) Pellecchia, M.; Bertini, I.; Cowburn, D.; Dalvit, C.; Giralt, E.; Jahnke, W.; James, T. L.; Homans, S. W.; Kessler, H.; Luchinat, C.; et al. Perspectives on NMR in drug discovery: a technique comes of age. *Nat. Rev. Drug Discovery* **2008**, *7* (9), 738−745.
(59) Dalvit, C. NMR methods in fragment screening: theory and a comparison with other biophysical techniques. *Drug Discovery Today* **2009**, *14* (21−22), 1051−1057.

https://doi.org/10.1021/acschembio.4c00259
ACS Chem. Biol. 2024, 19, 1852−1867

(60) Dubský, P.; Dvořák, M.; Ansorge, M. Affinity capillary electrophoresis: the theory of electromigration. *Anal. Bioanal. Chem.* **2016**, *408*, 8623−8641.
(61) Krylov, S. N. Kinetic CE: foundation for homogeneous kinetic affinity methods. *Electrophoresis* **2007**, *28* (1−2), 69−88.
(62) Chu, Y. H.; Whitesides, G. M. Affinity Capillary Electrophoresis Can Simultaneously Measure Binding Constants of Multiple Peptides to Vancomycin. *J. Org. Chem.* **1992**, *57* (13), 3524−3525.
(63) Gomez, F. A.; Avila, L. Z.; Chu, Y. H.; Whitesides, G. M. Determination of Binding Constants of Ligands to Proteins by Affinity Capillary Electrophoresis: Compensation for Electroosmotic Flow. *Anal. Chem.* **1994**, *66* (11), 1785−1791.
(64) Jameson, D. M.; Ross, J. A. Fluorescence polarization/anisotropy in diagnostics and imaging. *Chem. Rev.* **2010**, *110* (5), 2685−2708.
(65) Wolff, M. Polarization of light reflected from rough planetary surface. *Appl. Opt.* **1975**, *14* (6), 1395−1405.
(66) Jablonski, A. On the notion of emission anisotropy. *Bull. Acad. Polym. Sci.* **1960**, *8*, 259−264.
(67) Gradinaru, C. C.; Marushchak, D. O.; Samim, M.; Krull, U. J. Fluorescence anisotropy: from single molecules to live cells. *Analyst* **2010**, *135* (3), 452−459.
(68) Weber, G. Polarization of the fluorescence of macromolecules. I. Theory and experimental method. *Biochem. J.* **1952**, *51* (2), 145−155.
(69) *Synergy H1 Operator's Manual*. BioTek Instruments, Inc., 2012. https://www.lebonheur.org/research/investigator-resources/manuals/BioTek%20Synergy%20H1%20Hybrid%20Multi-Mode%20Plate%20Reader%20manual.pdf (accessed 2024-03-09).
(70) *Omega Series Operating Manual*. BMG LABTECH, 2017. https://med-fom-avgaylab.sites.olt.ubc.ca/files/2018/04/0415B0001K-Operating-Manual-Omega.pdf (accessed 2024-03-09).
(71) Clark, S. M.; Konermann, L. Determination of ligand-protein dissociation constants by electrospray mass spectrometry-based diffusion measurements. *Anal. Chem.* **2004**, *76* (23), 7077−7083.
(72) Jensen, H.; Østergaard, J. Flow induced dispersion analysis quantifies noncovalent interactions in nanoliter samples. *J. Am. Chem. Soc.* **2010**, *132* (12), 4070−4071.
(73) Bielejewska, A.; Bylina, A.; Duszczyk, K.; Fiałkowski, M.; Hołyst, R. Evaluation of ligand-selector interaction from effective diffusion coefficient. *Anal. Chem.* **2010**, *82* (13), 5463−5469.
(74) Clark, S. M.; Leaist, D. G.; Konermann, L. Taylor dispersion monitored by electrospray mass spectrometry: a novel approach for studying diffusion in solution. *Rapid Commun. Mass Spectrom.* **2002**, *16* (15), 1454−1462.
(75) Griffiths, A. On the movement of a coloured index along a capillary tube, and its application to the measurement of the circulation of water in a closed circuit. *Proc. Phys. Soc.* **1910**, *23* (1), 190.
(76) Taylor, G. I. Dispersion of soluble matter in solvent flowing slowly through a tube. *Proc. R. Soc. London Ser. A. Math. Phys. Sci.* **1953**, *219* (1137), 186−203.
(77) Trumbore, C. N.; Grehlinger, M.; Stowe, M.; Keleher, F. M. Further experiments on a new, fast method for determining molecular weights of diffusing species in a liquid phase. *J. Chromatogr. A* **1985**, *322*, 443−454.
(78) Wang, T. Y.; Rukundo, J.-L.; Le, A. T.; Ivanov, N. A.; Le Blanc, J. Y.; Gorin, B. I.; Krylov, S. N. Transient Incomplete Separation of Species with Close Diffusivity to Study the Stability of Affinity Complexes. *Anal. Chem.* **2022**, *94* (44), 15415−15422.
(79) Rukundo, J.-L.; Kochmann, S.; Wang, T. Y.; Ivanov, N. A.; Le Blanc, J. Y.; Gorin, B. I.; Krylov, S. N. Template Instrumentation for "Accurate Constant via Transient Incomplete Separation. *Anal. Chem.* **2021**, *93* (34), 11654−11659.
(80) Rukundo, J.-L.; Le Blanc, J. Y.; Kochmann, S.; Krylov, S. N. Assessing Accuracy of an Analytical Method in silico: Application to "Accurate Constant via Transient Incomplete Separation"(ACTIS). *Anal. Chem.* **2020**, *92* (17), 11973−11980.
(81) Schulte, J.; Tants, J.-N.; von Ehr, J.; Schlundt, A.; Morgner, N. Determination of dissociation constants via quantitative mass spectrometry. *Front. Anal. Sci.* **2023**, *3*, 1119489.
(82) Kempen, E. C.; Brodbelt, J. S. A method for the determination of binding constants by electrospray ionization mass spectrometry. *Anal. Chem.* **2000**, *72* (21), 5411−5416.
(83) Rinken, T.; Rinken, A.; Tenno, T.; Järv, J. Calibration of glucose biosensors by using pre-steady state kinetic data. *Biosens. Bioelectron.* **1998**, *13* (7−8), 801−807.
(84) Canbay, H. S. Spectrophotometric determination of acid dissociation constants of some arylpropionic acids and arylacetic acids in acetonitrile-water binary mixtures at 25°C. *Braz. J. Pharm. Sci.* **2022**, *58*, No. e20740.
(85) Van de Weert, M.; Stella, L. Fluorescence quenching and ligand binding: A critical discussion of a popular methodology. *J. Mol. Struct.* **2011**, *998* (1−3), 144−150.
(86) Andrus, A.; Bloch, W. HPLC of oligonucleotides and polynucleotides. *HPLC Macromol.* **1998**, *872*, 141.
(87) Raynal, B.; Lenormand, P.; Baron, B.; Hoos, S.; England, P. Quality assessment and optimization of purified protein samples: why and how? *Microb. Cell Fact.* **2014**, *13*, 180.
(88) Bange, A.; Halsall, H. B.; Heineman, W. R. Microfluidic immunosensor systems. *Biosens. Bioelectron.* **2005**, *20* (12), 2488−2503.
(89) Saha, S. *Performing Pipette Calibration Yourself*. Bitesize Bio, 2021. https://bitesizebio.com/40766/performing-pipette-calibration-yourself/ (accessed 2024-03-18).
(90) Berezovski, M.; Drabovich, A.; Krylova, S. M.; Musheev, M.; Okhonin, V.; Petrov, A.; Krylov, S. N. Nonequilibrium capillary electrophoresis of equilibrium mixtures: A universal tool for development of aptamers. *J. Am. Chem. Soc.* **2005**, *127* (9), 3165−3171.
(91) Bornhop, D. J.; Latham, J. C.; Kussrow, A.; Markov, D. A.; Jones, R. D.; Sørensen, H. S. Free-solution, label-free molecular interactions studied by back-scattering interferometry. *Science* **2007**, *317* (5845), 1732−1736.
(92) Latham, J. C.; Stein, R. A.; Bornhop, D. J.; Mchaourab, H. S. Free-solution Label-free Detection of α-Crystallin Chaperone Interactions by Back-scattering Interferometry. *Anal. Chem.* **2009**, *81* (5), 1865−1871.
(93) Stenberg, E.; Persson, B.; Roos, H.; Urbaniczky, C. Quantitative determination of surface concentration of protein with surface plasmon resonance using radiolabeled proteins. *J. Colloid Interface Sci.* **1991**, *143* (2), 513−526.
(94) Blackburn, C.; Sullivan, M. V.; Wild, M. I.; O'Connor, A. J.; Turner, N. W. Utilisation of molecularly imprinting technology for the detection of glucocorticoids for a point of care surface plasmon resonance (SPR) device. *Anal. Chim. Acta* **2024**, *1285*, 342004.
(95) Stahelin, R. V. Surface plasmon resonance: A useful technique for cell biologists to characterize biomolecular interactions. *Mol. Biol. Cell* **2013**, *24* (7), 883−886.
(96) Gasse, C.; Zaarour, M.; Noppen, S.; Abramov, M.; Marlière, P.; Liekens, S.; De Strooper, B.; Herdewijn, P. Modulation of BACE1 activity by chemically modified aptamers. *ChemBioChem.* **2018**, *19* (7), 754−763.
(97) Apiyo, D. O. Biolayer Interferometry (Octet) for Label-free Biomolecular Interaction Sensing. In *Handbook of Surface Plasmon Resonance*, 2nd ed.; Schasfoort, R. B. M., Ed.; Royal Society of Chemistry: London, UK, 2017; pp 356−397.
(98) Sultana, A.; Lee, J. E. Measuring protein-protein and protein-nucleic acid interactions by biolayer interferometry. *Curr. Protoc. Protein Sci.* **2015**, *79* (1), 19−25.
(99) Petersen, R. L. Strategies using bio-layer interferometry biosensor technology for vaccine research and development. *Biosensors* **2017**, *7* (4), 49.
(100) Friguet, B.; Chaffotte, A. F.; Djavadi-Ohaniance, L.; Goldberg, M. E. Measurements of the true affinity constant in solution of antigen-antibody complexes by enzyme-linked immunosorbent assay. *J. Immunol. Methods* **1985**, *77* (2), 305−319.

https://doi.org/10.1021/acschembio.4c00259
ACS Chem. Biol. 2024, 19, 1852−1867

(101) Orosz, F.; Ovádi, J. A simple method for the determination of dissociation constants by displacement ELISA. *J. Immunol. Methods* **2002**, *270* (2), 155−162.
(102) Kim, B.; Dikova, E.; Sheller, U.; Dikov, M.; Gavrilova, E.; Egorov, A. Evaluation of dissociation constants of antigen-antibody complexes by ELISA. *J. Immunol. Methods* **1990**, *131* (2), 213−222.
(103) Ekins, R. P.; Newman, G. B.; Piyasena, R.; Banks, P.; Slater, J. D. H. The radioimmunoassay of aldosterone in serum and urine: Theoretical and practical aspects. *J. Steroid Biochem.* **1972**, *3* (3), 289−304.
(104) Murthy, G.; Venkatesh, N. Determination of kinetic parameters of epitope-paratope interaction based on solid phase binding: An inexpensive alternate to biospecific interaction analysis. *J. Biosci.* **1996**, *21*, 641−651.
(105) Lessard, J. L.; Carlton, D.; Rein, D. C.; Akeson, R. A solid-phase assay for antiactin antibody and actin using protein-A. *Anal. Biochem.* **1979**, *94* (1), 140−149.
(106) Cottet, H.; Biron, J.-P.; Martin, M. Taylor dispersion analysis of mixtures. *Anal. Chem.* **2007**, *79* (23), 9066−9073.
(107) Lakowicz, J. R.; Lakowicz, J. R. Fluorescence anisotropy. In *Principles of fluorescence spectroscopy*; Springer, 1999; pp 291−319. DOI: 10.1007/978-1-4757-3061-6_10.
(108) Park, S.-H.; Raines, R. T. Fluorescence polarization assay to quantify protein-protein interactions. In *Protein-Protein Interactions: Methods and Applications*; Fu, H., Ed.; Humana Press, 2004; pp 161−165. DOI: 10.1385/1-59259-762-9:161.
(109) Nosjean, O.; Souchaud, S.; Deniau, C.; Geneste, O.; Cauquil, N.; Boutin, J. A. A simple theoretical model for fluorescence polarization binding assay development. *SLAS Discovery* **2006**, *11* (8), 949−958.
(110) Yan, K.; Hunt, E.; Berge, J.; May, E.; Copeland, R. A.; Gontarek, R. R. Fluorescence polarization method to characterize macrolide-ribosome interactions. *Antimicrob. Agents Chemother.* **2005**, *49* (8), 3367−3372.
(111) Liao, J.-y.; Song, Y.; Liu, Y. A new trend to determine biochemical parameters by quantitative FRET assays. *Acta Pharmacol. Sin.* **2015**, *36* (12), 1408−1415.
(112) Liu, J.; Lu, Y. FRET study of a trifluorophore-labeled DNAzyme. *J. Am. Chem. Soc.* **2002**, *124* (51), 15208−15216.
(113) Sebille, B.; Zini, R.; Madjar, C.-V.; Thuaud, N.; Tillement, J.-P. Separation procedures used to reveal and follow drug-protein binding. *J. Chromatogr. B: Biomed. Sci. Appl.* **1990**, *531*, 51−77.
(114) Lowe, E. A.; Lu, M.; Wang, A.; Cortez, H.; Ellis, D.; Liu, X. C. Stationary phase-based two-dimensional chromatography combining both covalent and noncovalent interactions on a single HPLC column. *J. Sep. Sci.* **2006**, *29* (7), 959−965.
(115) Equations Used for Fitting ITC Data. *ITC Data Analysis in Origin - Tutorial Guide*; MicroCal: Northampton, MA, 2004; pp 104−108.
(116) Neves, M. A. D.; Slavkovic, S.; Churcher, Z. R.; Johnson, P. E. Salt-mediated two-site ligand binding by the cocaine-binding aptamer. *Nucleic Acids Res.* **2017**, *45* (3), 1041−1048.
(117) Neves, M. A. D.; Shoara, A. A.; Reinstein, O.; Abbasi Borhani, O.; Martin, T. R.; Johnson, P. E. Optimizing Stem Length To Improve Ligand Selectivity in a Structure-Switching Cocaine-Binding Aptamer. *ACS Sens.* **2017**, *2* (10), 1539−1545.
(118) Baaske, P.; Wienken, C. J.; Reineck, P.; Duhr, S.; Braun, D. Optical thermophoresis for quantifying the buffer dependence of aptamer binding. *Angew. Chem., Int. Ed.* **2010**, *49* (12), 2238−2241.
(119) El-Hawiet, A.; Kitova, E. N.; Arutyunov, D.; Simpson, D. J.; Szymanski, C. M.; Klassen, J. S. Quantifying ligand binding to large protein complexes using electrospray ionization mass spectrometry. *Anal. Chem.* **2012**, *84* (9), 3867−3870.
(120) Jafari, M. R.; Deng, L.; Kitov, P. I.; Ng, S.; Matochko, W. L.; Tjhung, K. F.; Zeberoff, A.; Elias, A.; Klassen, J. S.; Derda, R. Discovery of light-responsive ligands through screening of a light-responsive genetically encoded library. *ACS Chem. Biol.* **2014**, *9* (2), 443−450.
(121) Tjernberg, A.; Carnö, S.; Oliv, F.; Benkestock, K.; Edlund, P.-O.; Griffiths, W. J.; Hallén, D. Determination of dissociation constants for protein-ligand complexes by electrospray ionization mass spectrometry. *Anal. Chem.* **2004**, *76* (15), 4325−4331.
(122) Rabenstein, D. L.; Sayer, T. L. Determination of microscopic acid dissociation constants by nuclear magnetic resonance spectrometry. *Anal. Chem.* **1976**, *48* (8), 1141−1146.
(123) Shoara, A. A.; Churcher, Z. R.; Slavkovic, S.; Johnson, P. E. Weak Binding of Levamisole by the Cocaine-Binding Aptamer Does Not Interfere with an Aptamer-Based Detection Assay. *ACS Omega* **2021**, *6* (37), 24209−24217.
(124) Johnson, P. E.; Tomme, P.; Joshi, M. D.; McIntosh, L. P. Interaction of soluble cellooligosaccharides with the N-terminal cellulose-binding domain of Cellulomonas fimi CenC. 2. NMR and ultraviolet absorption spectroscopy. *Biochemistry* **1996**, *35* (44), 13895−13906.
(125) Fushman, D.; Cahill, S.; Cowburn, D. The main-chain dynamics of the dynamin pleckstrin homology (PH) domain in solution: analysis of 15N relaxation with monomer/dimer equilibration. *J. Mol. Biol.* **1997**, *266* (1), 173−194.
(126) Monasterio, O. Rate Constants Determined by Nuclear Magnetic Resonance. *Methods* **2001**, *24* (2), 97−103.
(127) Fried, M. G. Measurement of protein-DNA interaction parameters by electrophoresis mobility shift assay. *Electrophoresis* **1989**, *10* (5−6), 366−376.
(128) Hellman, L. M.; Fried, M. G. Electrophoretic mobility shift assay (EMSA) for detecting protein-nucleic acid interactions. *Nat. Protoc.* **2007**, *2* (8), 1849−1861.
(129) Hsieh, Y.-W.; Alqadah, A.; Chuang, C.-F. An optimized protocol for electrophoretic mobility shift assay using infrared fluorescent dye-labeled oligonucleotides. *J. Vis. Exp.* **2016**, No. 117, No. e54863.
(130) Hummel, J.; Ver Ploeg, D. A.; Nelson, C. A. The interaction between ribonuclease and mononucleotides as measured spectrophotometrically. *J. Biol. Chem.* **1961**, *236* (12), 3168−3172.
(131) Hummel, J. P.; Dreyer, W. Measurement of protein-binding phenomena by gel filtration. *Biochim. Biophys. Acta* **1962**, *63* (3), 530−532.

https://doi.org/10.1021/acschembio.4c00259
ACS Chem. Biol. 2024, 19, 1852−1867